A THEORETICAL INVESTIGATION OF A CIRCULAR LIFTING JET IN A CROSS-FLOWING MAINSTREAM

J. E. Hackett
H. R. Miller

FOREWORD

The research described here was conducted by the Lockheed-Georgia Company under Contract F33615-69-C-1753 for the Air Force Flight Dynamics Laboratory, AFSC, Wright-Patterson Air Force Base, Ohio, with Mr. R. F. Osborn (FXM) as Project Engineer. This work was initiated under Project No. 6169BT, V/STOL Aerodynamics.

The studies were concluded in December 1970, and this report was released by the authors in January 1971 as an R & D Technical Report. (For internal purposes only, this report has been designated Lockheed-Georgia Company Report No. ER-10940.)

This technical report has been reviewed and is approved.

P. P. ANTONATOS
Chief, Flight Mechanics Division
Air Force Flight Dynamics Laboratory

ABSTRACT

Finite-element potential-flow-modeling theoretical techniques are described which predict, from first principles, both the rolled-up geometry and the path of a round lifting jet emergent into a cross-flowing mainstream, as on VTOL or direct lift-assisted STOL aircraft. Starting with a straight-cylinder geometry, "point" vortex elements are perturbed using a predictor-corrector stepping method to give a first estimate of the bent-back shape, using assumed circulation values. A collocation scheme is next used to revise the circulation values, and after three or four iterations, a final exit-plane pressure distribution may be calculated. The fan-induced total pressure rise is simulated by injecting vortex rings at a chosen position in the duct which feeds the jet. Since the scope of the method is entirely non-viscous, separations toward the rear of real jets and the associated pressure changes are not simulated and base-pressure type of pressures cannot be expected. Nevertheless, for forward speed ratios of 0.1, 0.2, 0.3 and 0.4, the low-pressure contours at each side of the jet do show an increasing rearward shift, just as is found experimentally. Somewhat surprisingly, the simulated plumes were more stable at higher velocity ratios. At lower forward speeds, there was a tendency to flap, rather like a hose end when freed. It is anticipated that, if viscous effects were simulated, these motions might damp out.

TABLE OF CONTENTS

TABLE OF CONTENTS (Continued)

LIST OF ILLUSTRATIONS

LIST OF SYMBOLS

CX, CY, CZ	resultant short element circulation components.
CXR, CYR, CZR	ring short element circulation components.
CXT, CYT, CZT	trailer short element circulation components.
d_i	normalized deviation of short element from true position.
DRING	circumferential pitch of short elements.
DZ	axial pitch of short elements
F	force acting on short element
H	total head of fan.
H_P	initial length of plume below exit plane.
K	circulation strength
N_M	maximum number of short elements in system.
N_R	number of short elements per ring.
P	static pressure.
P_∞	mainstream ambient pressure.
R	jet orifice or duct radius.
R_L	distance between vortex element and calculation point.
t	time.
T_M	maximum number of time-steps.
U, V, W	induced velocity components.
V_∞, VO	mainstream velocity
W_J, WJ	jet velocity.
W_R	ring vortex convection velocity.
X, Y, Z	Cartesian coordinates.
ρ	density.
θ	peripheral angle subtended by ring vortex element.
φ_1, φ_2, φ_3	direction cosines at collocation points.

SECTION I

INTRODUCTION

For more than the 10 years that higher-disc-loading VTOL aircraft have been flying, it has been realized that serious lift losses and pitching moments occur at forward speed for some lift-jet geometries, particularly those with large exposed horizontal areas aft of the jet exit. Measurements by Bradbury and Wood[1] and Vogler[2] show the lobes of low-surface pressure in the quadrants behind a vertical jet that are responsible for the adverse effects. Early work by Jordinson[3] demonstrated the formation of a vortex pair as the jet turns towards the mainstream direction; the forces aft of the jet are associated with the jet's change of direction. A reliable means of predicting these forces is urgently needed.

Margason[4] and others have measured mean jet paths for various jet velocities and emergence angles into the mainstream. In a number of theoretical treatments, Margasson's (or similar) measurements have been used as a starting point for methods involving sources, sinks, or vortex lines distributed about the mean line, often in a somewhat arbitrary manner. Another approach involves assigning "drag coefficients" to jet cross-sections along the plume, but this involves obvious conceptual difficulties. In application to a practical design problem, all of these suffer from the weakness that the jet path generally is not known a priori. Excessive computer demands can arise, particularly with vortex lattice methods, when large numbers of elements are used to describe even one jet. Line singularities in three dimensions, associated with vortices used for flow modeling, are a constant numerical hazard, particularly if perturbation methods are also used. Extensive references to these and other methods are present in Reference 5.

At the suggestion of L. Prandtl in the early 1940's, H. C. Lu studied the theoretical deformation of a two-dimensional circular cylinder, with time, using concentrated vortices of appropriate strengths distributed around the periphery.[6] She calculated at each vortex the sums of velocity components due to the mainstream and induced by the other vortices. This velocity was assumed constant during a short time step, and displacements were calculated to yield a new set of vortex positions. Repetition for 30 to 40 time steps gave a rolled-up geometry which resembles the downstream end of a jet in a cross-flow. In Lu's model, an equivalence between jet direction and time was rigidly adhered to, giving a jet structure similar to that we calculated recently (Figure 1). Here, the cylinder cross-sections associated with increasing total times are shown as horizontal planes stacked below one another. This two-dimensions-plus-time analog takes into account neither mutual induction effects across horizontal planes nor the ring-vortex-sheet which defines the edge of the jet. Excessive jet penetration results, even for the low forward speeds specified by the original author.

The essentially three-dimensional nature of the jet-plume and mainstream interaction is illustrated by Figure 2. Rolling-up vortices can be seen which extend from the jet orifice to form a trailing pair far downstream. Figure 3 shows corresponding sketches which illustrate the structure more explicitly. (Further description may be found on page 31 of Reference 5.)

The method described here extends the work of H. C. Lu to a fully three-dimensional perturbation method that includes a ring vortex system and that takes into account interactions with nearby surfaces, including the duct itself. The aim is to predict jet path and cross-sectional structure in sufficient detail to predict well the pressures on nearby surfaces, while avoiding as many as possible of the pitfalls mentioned in the second paragraph, above. In the treatment here, viscous effects are entirely neglected; the addition of these effects could be the subject of future work.

Though oriented towards VTOL, there are several STOL and other applications for the methods described here. The most obvious is the application to direct-lift-assisted STOL vehicles. However, perhaps more important than this is the fact that powered free flows are being treated. The understanding gained, and some of the methods, could ultimately be used in a broader range of applications, including other STOL configurations. The most immediately accessible problem is slipstream contraction over wings, and some of the methods described here will shortly be applied to this. Probably the most difficult flow to treat would be that between a ducted-fan engine and an externally blown flap.

In the following section, the theory used will be described in more detail and some underlying theoretical results will be presented. Implementation in the form of algorithms for a digital computer will be described in Sections III and IV. Numerical accuracy and stability considerations of the modeling technique are discussed in Section V. Our final results will be described in Section VI, and conclusions in Section VII.

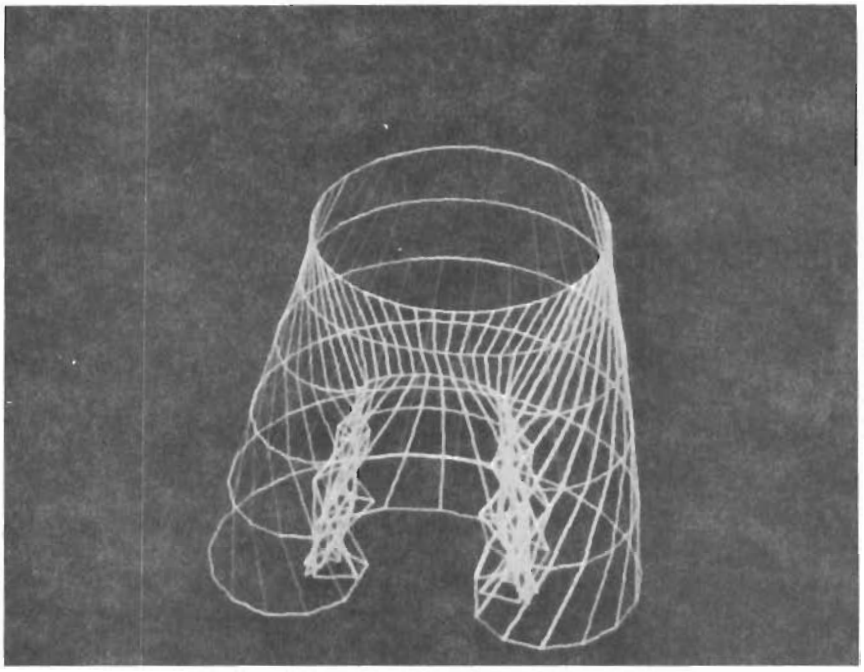

FIGURE 1. COMPUTER-GRAPHIC DISPLAY OF THE RESULTS OF AN H. C. Lu TYPE OF CALCULATION.

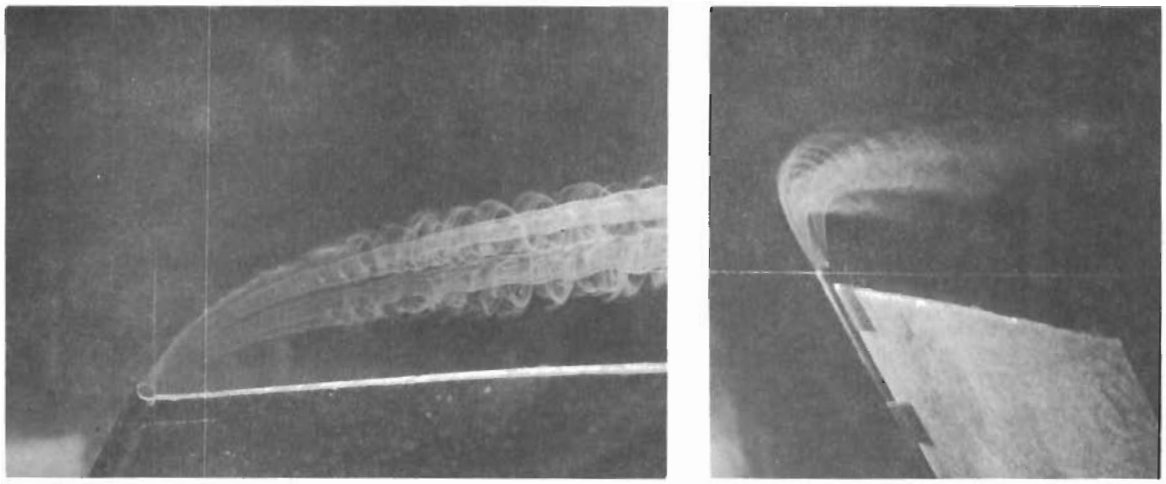

FIGURE 2. A LOW REYNOLDS NUMBER SMOKE JET

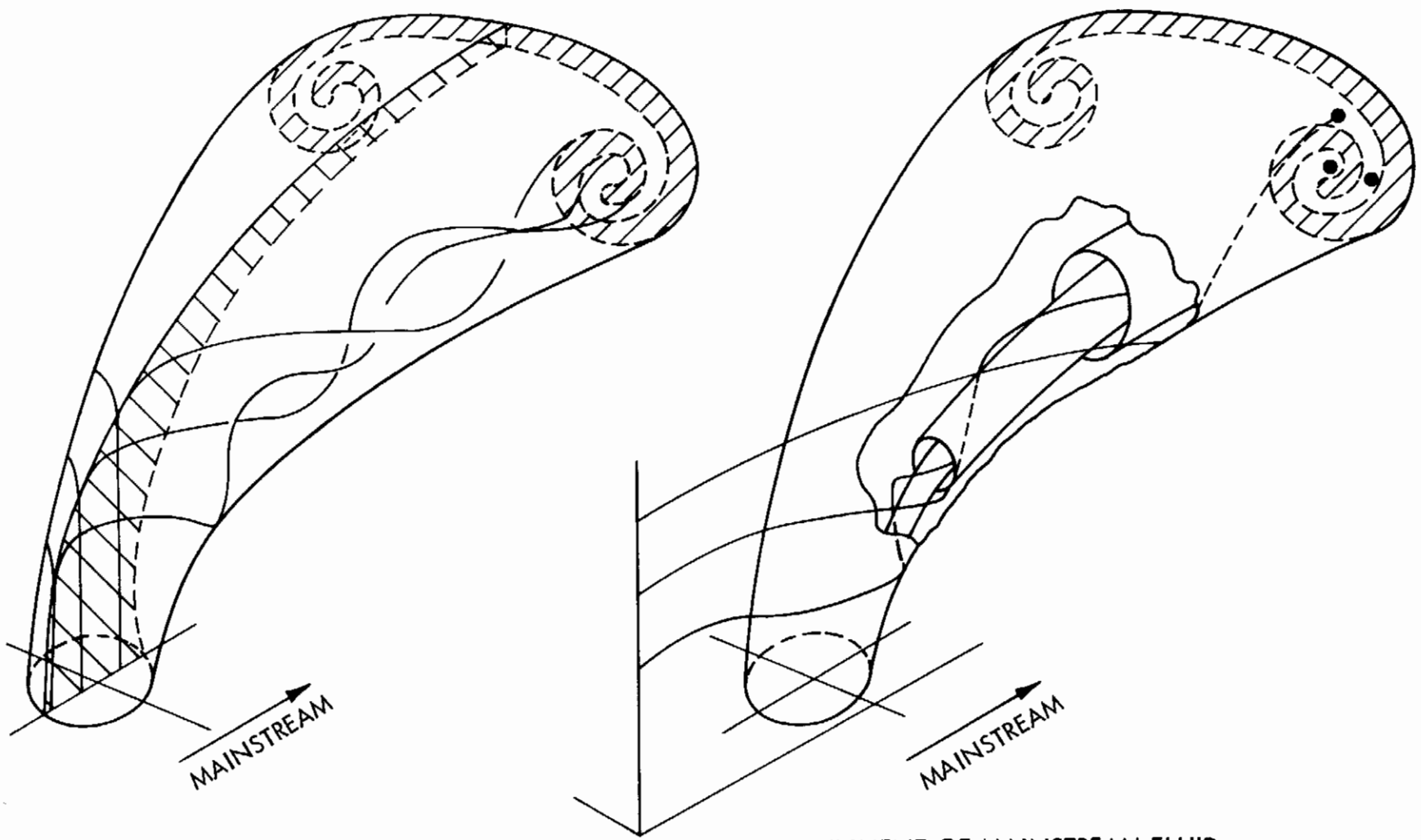

DISTORTION OF JET FLUID

ENTRAINMENT OF MAINSTREAM FLUID

FIGURE 3. THE FORMATION OF TRAILING VORTICES.

SECTION II

DISCUSSION AND GENERAL APPROACH

1. THE COMPONENT FLOWS

a. Two Classical Results

In Appendix I it is shown that there is no motion outside a doubly infinite ring-vortex cylinder, and no motion inside a cylinder placed normal to a mainstream, provided each is represented by a distribution of surface vortices. Therefore, if the two vortex systems coexist on a single cylinder, the flows they induce do not interfere with each other. Consequently, this is a very suitable vortex geometry for use as a starting condition in a perturbation solution in three dimensions, analogous to H. C. Lu's treatment discussed above.

The above potential-flow properties can be related to the geometry of the duct and exit surfaces. Flow outside the cylinder is "horizontal" so that an "exit plane" may be placed at any z position and will have zero flow through it. Equally, since all the flow inside is "vertical," a supply duct leading to the exit plane may be envisaged which will have no flow through its walls. Neither net lift nor moment is induced on the exit plane in this initial condition, and the duct experiences zero drag at each axial position. The interference forces and moments, associated with jet bending and roll-up, can thus be identified as secondary effects, albeit strong ones.

b. Flows of Differing Total Pressure

No mention has yet been made of the relative strengths of the ring and longitudinal vortex sheets. For a given mainstream speed, V_∞, the longitudinal vortex strength distribution is defined. If both vortex systems are stationary, no energy can be added to the flow, and the total pressures inside and outside will be equal. This restricts the ring vortex strength to a value corresponding to equal mainstream and jet velocities. A means for representing energy addition is needed which is equivalent to a fan.

Figure 4 shows a section of circular duct, containing uniform flow at velocity W_j. A fan is situated on plane "A," and we assume that the duct exhausts at the ambient static pressure (p_∞) so that flow leaves the exit in a parallel manner. For this to happen, it also follows that rings to the right of A, at least, must convect at the self-induced speed, $(1/2)W_J$. Conditions downstream of the fan are now defined. Upstream of the fan, the absolute pressure if $(p_\infty - \Delta P)$, where ΔP $(= \Delta H)$ is the pressure rise imparted by the fan. An inward force on the duct walls upstream is implied which, in turn, implies that ring vortices there must move at less than their natural convection speed.

If W_R is the convection speed of vortices to the left of A, the velocity of flow passing over them is $\left[1/2(\partial K/\partial z) - W_R\right]$ and the force, dF, experienced by an element of dz becomes

$$dF = \rho \left(\frac{1}{2}\frac{\partial K}{\partial z} - W_R\right)\left(\frac{\partial K}{\partial z}\,dz\right) R \quad d\theta$$

or

$$\frac{dF}{R\ d\theta dz} = \Delta P = \Delta H = \frac{1}{2}\rho\, W_J(W_J - 2W_R) \qquad (1)$$

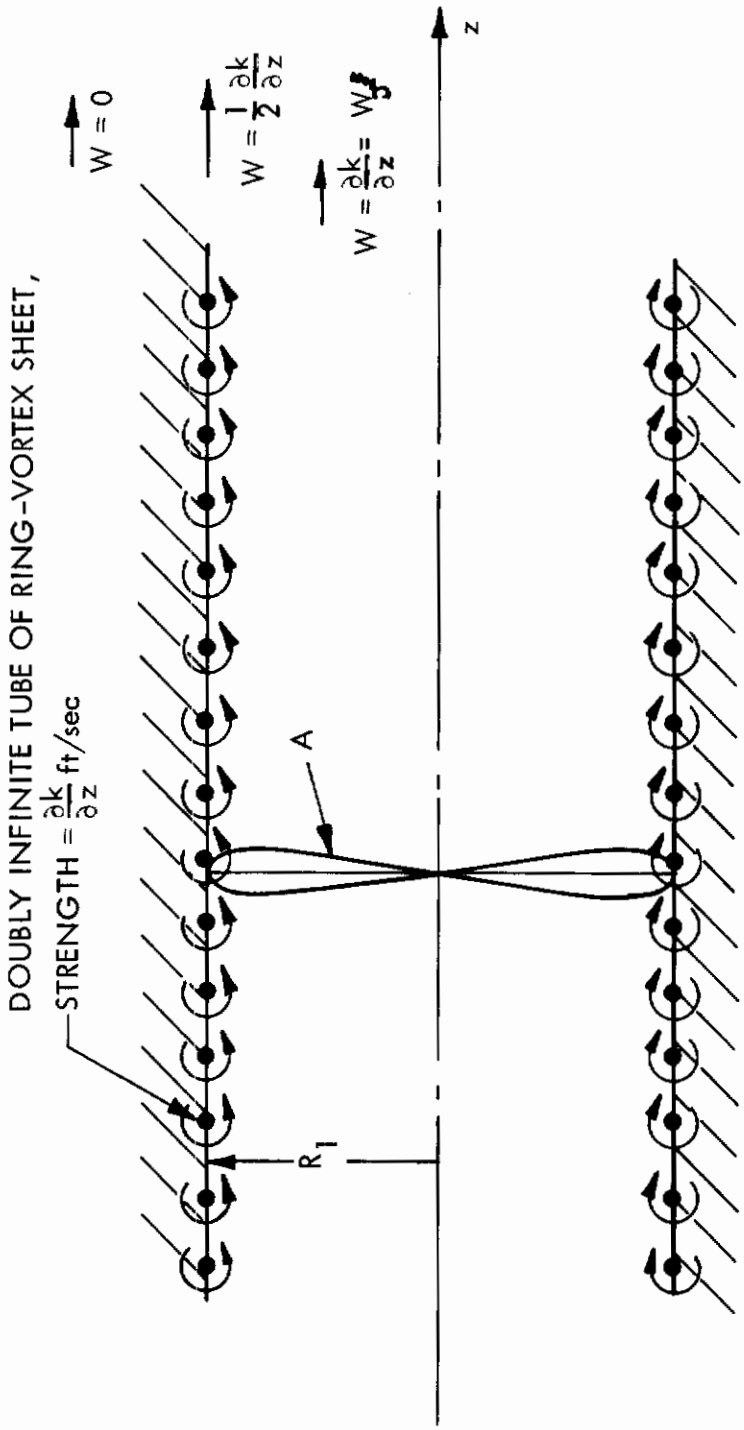

FIGURE 4 SIMULATION OF FAN TOTAL-PRESSURE RISE

If the duct intake air has mainstream total pressure equal to $\left(p_\infty + \frac{1}{2}\rho V_\infty^2\right)$, as in a practical case, and the exit total pressure is $\left(p_\infty + \frac{1}{2}\rho W_J^2\right)$, then

$$\Delta H = \frac{1}{2}\rho W_J^2 - \frac{1}{2}\rho V_\infty^2 = \frac{1}{2}\rho W_J^2 - \rho W_J W_R \qquad \text{from (1)}$$

$$\therefore \quad W_J W_R = \frac{1}{2} V_\infty^2$$

$$\frac{W_R}{W_J} = \frac{1}{2}\left(\frac{V_\infty}{W_J}\right)^2 \qquad (2)$$

for air taken at mainstream total pressure $\left(p_\infty + \frac{1}{2}\rho V_\infty^2\right)$.

If W_J equals V_∞, no energy addition is needed, and W_R assumes its "natural" value equal to half the jet speed. Otherwise, there is a change in the vortex sheet velocity at plane "A," and new vortex sheet must be fed in continuously. This is the means by which energy is added to the flow. We note that fan surface is defined only around the periphery of plane "A." Also, if V_∞ exceeds W_J, the mainstream would be driving the fan, and W_R would exceed $(1/2)W_J$, making necessary vortex sheet removal, corresponding to energy extraction from the flow.

Since treatment of the intake flows is beyond the scope of this report, the treatment of vortex rings upstream of the fan will not be extended further. Instead we shall consider a geometry with no vortex rings upstream of the fan, corresponding to a fan placed right at a duct entry. It is then necessary to constrain the rings radially to the duct walls, to prevent slipstream contraction. Peripheral and axial freedom should still be allowed, but for simplicity of programming, only the latter will be permitted. The ability to determine slipstream contraction shapes is implicit in the methods used, by specifying a duct of zero length.

c. The Downstream End of the Plume

For any calculation of the present type to stay within reasonable bounds, there must be vortex sheet removal at the downstream end of the plume equal to the injection at the fan. This removal corresponds to the total pressure decay which occurs in a real plume and, ideally, should be gradual, with the trailing vortices retained and streamed to downstream infinity. These refinements were not included in the current program, the approach being to use sufficient plume length for additional length at the downstream end to have little effect back at the exit. Thus, the nature of the solution remains purely potential flow, with no pseudo-viscous ring attenuation effects, at least so far as the exit is concerned.

2. FIXED AND MOVING VORTEX SYSTEMS

We have now discussed the major flow features and can describe the principal components of a solution to the problem. Reference has been made only to line vortices and vortex rings so far; doublet-type solutions have not been considered. There are two reasons: vortex lines may be interpreted in more nearly physical terms, and they are more economical for local flow effects like the current problem. For example, a vortex ring,

which is a line, is mathematically equivalent to a disc of doublets; this requires an area-type description and more integration points or sub-elements.

a. Duct, Exit Plane, and Ring Vortex Systems

Figure 5 shows the three vortex sheets which must be considered. The duct and exit vortex systems are fixed but have trailing sheets which join the moving ring-sheet and become free downstream of the exit. The exit pressure distribution will be reflected by the vortex strengths eventually determined in the exit plane. The duct pressure distribution will be determined similarly; we have seen no previous attempt to predict this.

A ring-vortex sheet, injected at the fan position (which can be chosen), will self-propagate down the duct when perturbation is started, radial constraint being applied. Since the fixed (duct) sheet lies in the same surface, there is an immediate problem regarding singularities, regardless of whether a continuous or a discrete solution is used. (Details of how this is handled are discussed in Section III.)

b. Boundary Conditions at "Hard" Surfaces

The term "hard surfaces" will be used here to identify surfaces at which zero normal flow is imposed, to distinguish them from "free surfaces" like those of the jet plume itself.

One of the less obvious features of the problem is how to treat the exit plane properly. Because of the exit hole, the simple reflection techniques which were first considered appear to be inappropriate, and attempts to find a suitable modification proved fruitless. It was then obvious that the boundary conditions would have to be enforced over both exit and duct surfaces, a step taken with reluctance because of the potential impact on computer time. The problem has mixed boundary conditions: free surface at the plume and hard surfaces on the duct and on the exit plane, with a joining line along the duct periphery.

Two types of solution must be matched: a perturbation solution for the plume and a collocation-type solution, for example, for the "hard" surfaces. Though perturbation methods are demanding on computer time, the need for collocation points on the plume (for example, as illustrated on page 175 of Reference 5) is avoided. Less core storage is needed and only moderate sized influence matrices become involved, since trailing vortex strengths are determined at their upstream ends. The forcing functions are fairly complicated, since they contain not only mainstream components but also velocities induced by the fixed-strength ring-vortex sheet, which distorts with the plume.

3. VORTEX MODELING TECHNIQUES

The discussion so far applies equally for continuous-sheet and finite-element solutions. However, the nature of the boundary conditions encourages the latter, which also is a natural extension of earlier work. It is clear, nevertheless, that the use of line vortices may be hazardous because of the singularity problem, and alternative means were devised.

a. Singularities

When the problem is appropriately posed, the singularity in a continuous vortex sheet can become integrable. If we consider the idealized example of a flat, square plate having vortex lines distributed parallel to one edge, considerations of symmetry alone

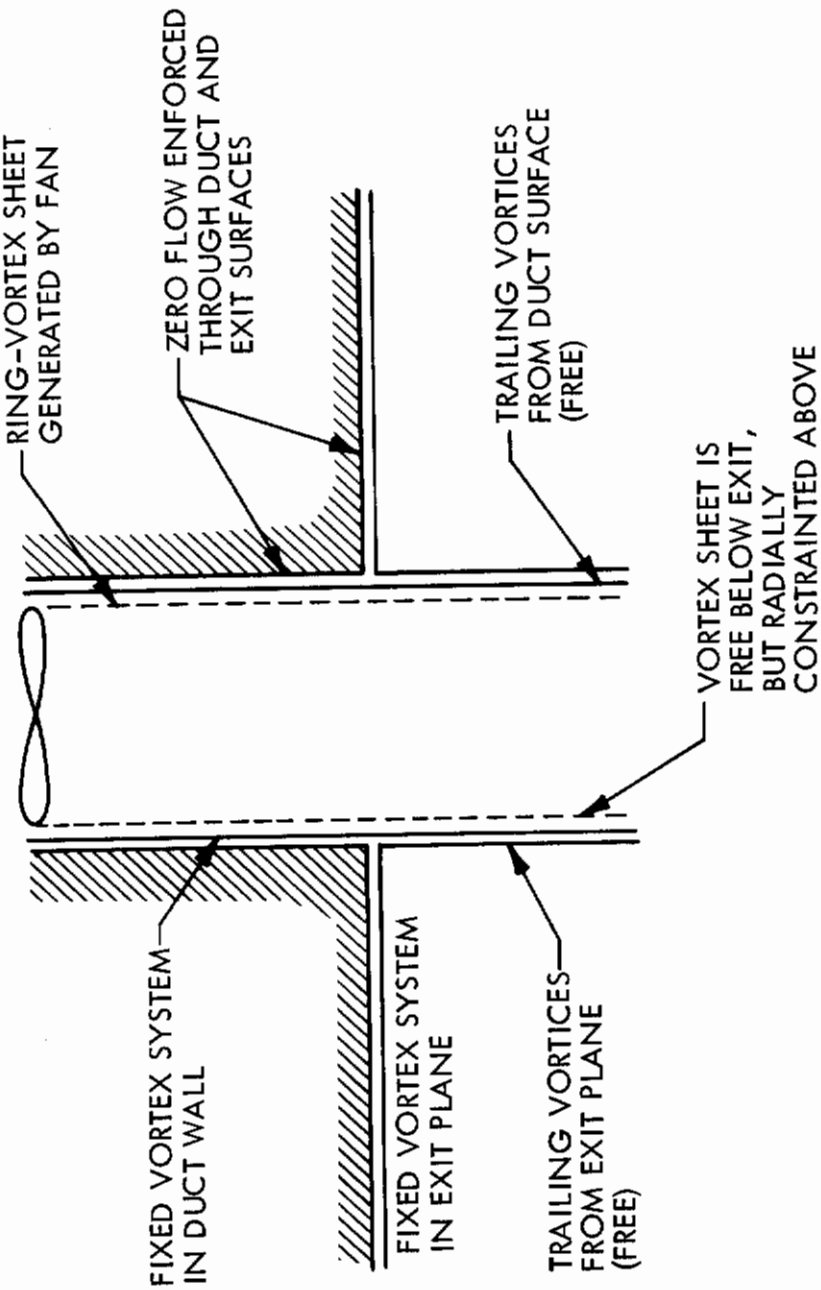

FIGURE 5 FIXED AND MOVING VORTEX SYSTEMS

show that zero normal velocity is induced at the center. There are singular lines along each of the edges parallel to the vortex direction, which condense to the familiar line singularity if a line vortex is used to represent the plate. Figure 6 illustrates both this effect and the velocities due to a point vortex element formed when the line vortex, in turn, is compressed to a point. The units of circulation strength are ft/sec, ft^2/sec, and ft^3/sec for the plate, line and point, respectively.

Within the plate boundary, neither the line nor the point can be expected to approach proper representation; the singularity is wrongly placed. Zero velocity is often assigned at point S when line or point representations are used, using logical computer algorithms. At P, opposite to the end of the line vortex and beyond it, zero velocity is obtained for the line and the point. However, the velocity gradient here is incorrect for the line; as frequently formulated, there is also a specious numerical singularity here.

At Q and R, the other likely nearby collocation positions, the line and the point approximations, respectively, give the better approximation to the solution for the plate. For larger distances, the three results converge quite rapidly.

The errors, averaged over P, Q, and R, are 0.0029 and 0.0018 for the line and point elements, respectively, in the units of Figure 6. There are further advantages for the point elements. The algorithms are very simple, since the point vector may be resolved into orthogonal strength components, and the point itself is the integrand element for continuous sheet treatments. Therefore, there is potential for later extensions to more sophisticated integration methods, which would include the effect, at S, of vortex strength gradients across the plate.

When used within a perturbation scheme, considerations arise both of continuity of vortex lines and of stretching, the latter because element area is implied in the definition of point strength. Appropriate reorientation and strength modification become necessary after each time step. When the programs described later were developed, these measures were initially left out. Their subsequent inclusion affected the stability of the calculation.

At the current stage of development, point elements released with uniform spacing around the duct exit are allowed to perturb, stretch, and reorient as they convect down the plume boundary. As this happens, some parts of the sheet become more densely populated than others; no attempt is made at redistribution. Such a refinement would be appropriate if more advanced integration schemes were to be applied. A mix of element types could also be contemplated.

b. Convection of a Ring Vortex Sheet

Since we shall be approximating a continuous ring-vortex sheet by point elements, it is important to arrange that the correct convection velocity is retained. There is little chance of a correct solution if this is neglected. Using Reference 7 as an initial guide, detailed studies were carried out of ring-vortex cylinders and their representation by finite elements. A closed-form analytical solution was determined for radial and axial velocity components at a general point, caused by a ring-vortex cylinder having a squarely cut-off end. Such a boundary condition generally cannot be described in terms of the spherical coordinates of Appendix I, part (ii), and considerable mathematical complication resulted. Though it was used for comparative purposes during studies of finite elements, a decision was made not to incorporate this solution into the main program.

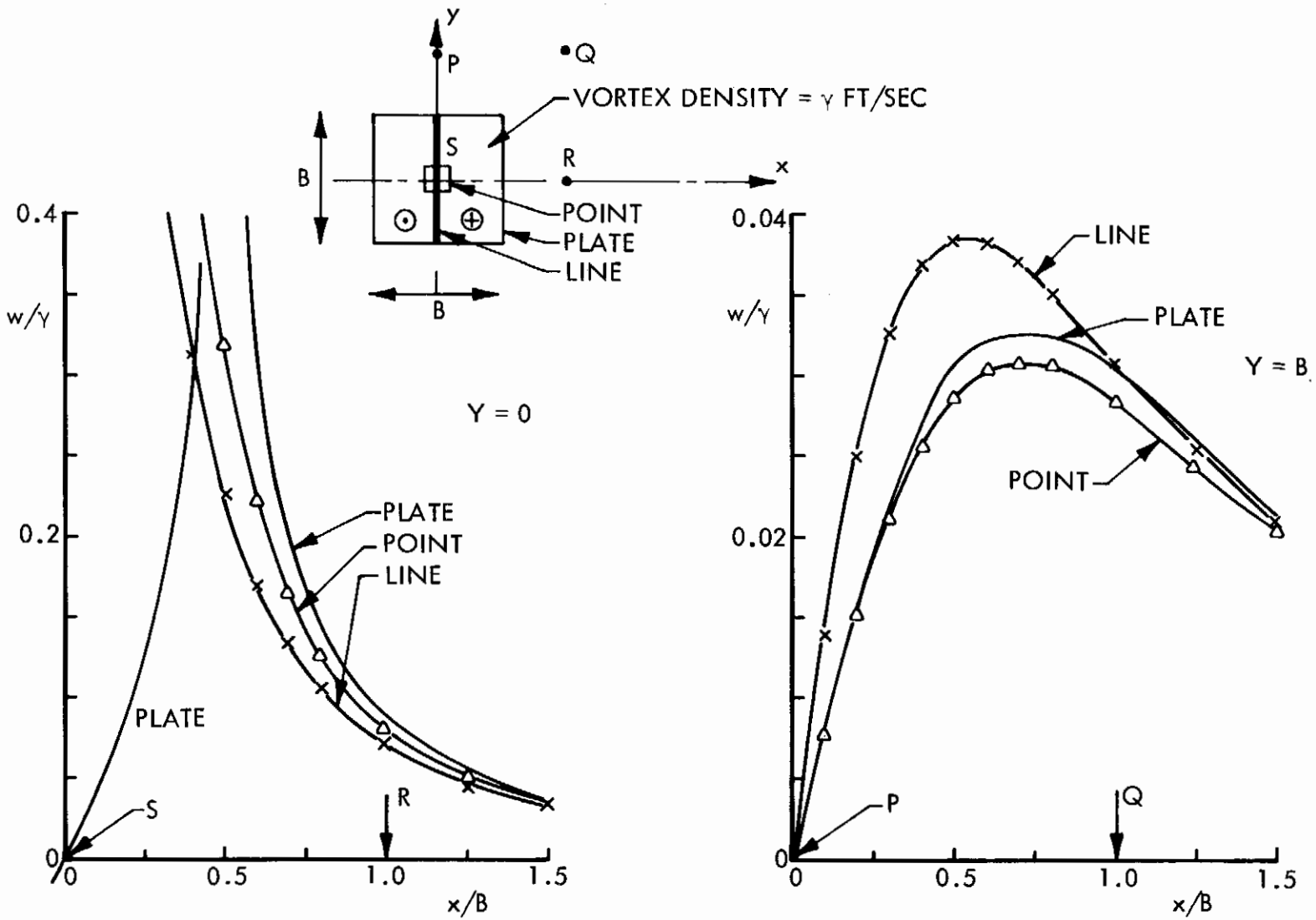

FIGURE 6. NORMAL VELOCITIES INDUCED BY THREE TYPES OF VORTEX ELEMENTS

Figure 7 shows a typical plot used during the element studies. Velocity calculations excluding and including the in-plane ring were made, to determine the size of errors which cancel. It should be noted that the limiting geometry as pitch becomes zero is not a ring-cylinder but vertical vortex lines with transverse vorticity. It may be shown that the corresponding convection velocity, for zero pitch, is $0.5(1 - 1/N_R)$. Clearly, serious errors result for small N_R. The figure shows how underestimated induction effects from out-of-plane are balanced by overestimated velocities due to in-plane elements to give correct convective velocity at one particular value of ring spacing. Figure 8a is a cross-plot of Figure 7 and shows values of pitch required to give correct convection velocity for various numbers of elements per ring. Generally, the axial spacing is significantly greater than the peripheral spacing.

Corresponding results are also shown for stacks of line-vortex polygons, calculated at the junctions (Figure 8b) and at mid-link positions (Figure 8c). Even greater axial spacings than for point elements are needed for the junction convective velocity to be correct, but at mid-link, only zero spacing gives the correct result. A good compromise position was found about a quarter of the way from either end, but for the reasons given previously this was not exploited.

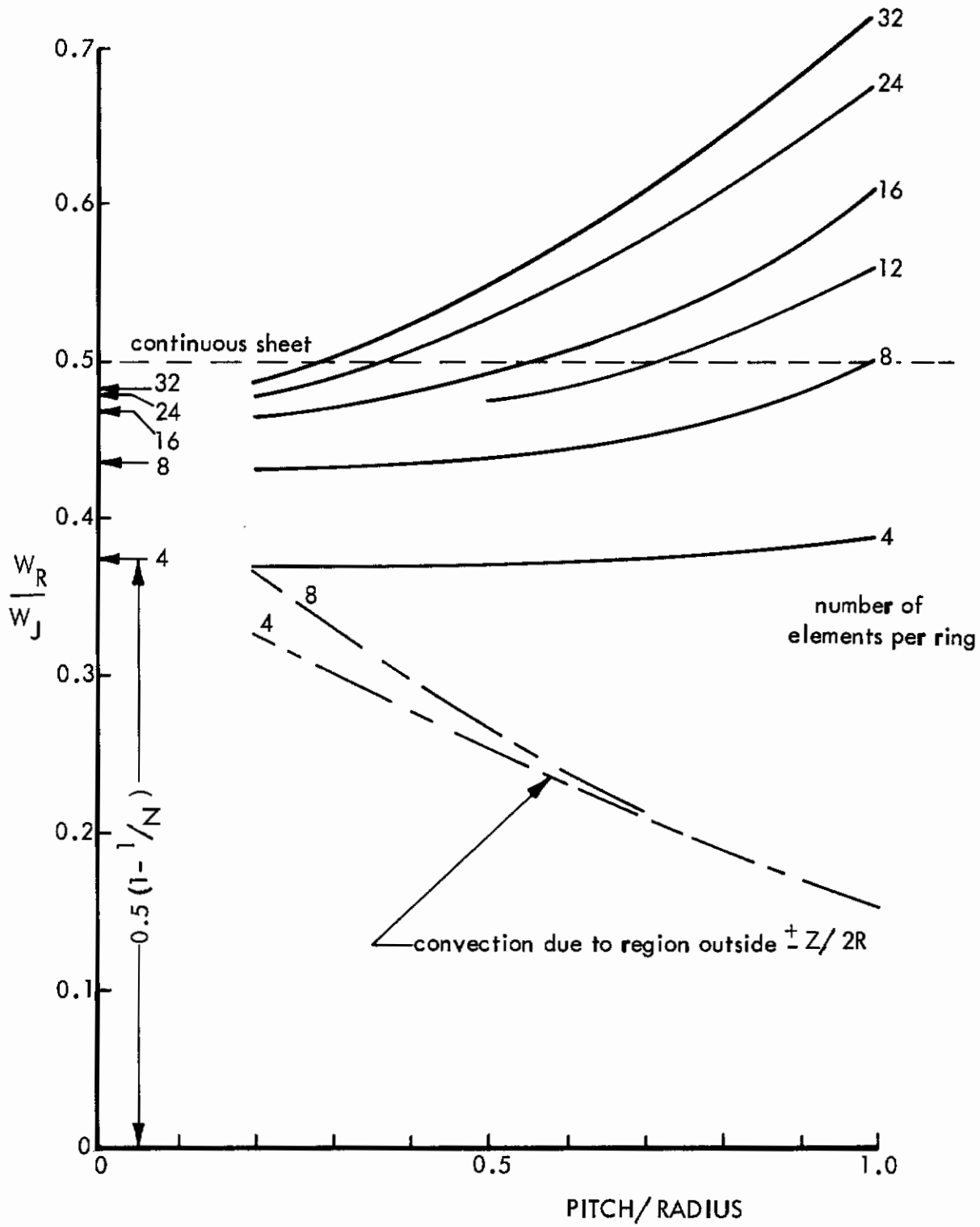

FIGURE 7. VARIATION OF RING-CYLINDER SELF-CONVECTION VELOCITY WITH GEOMETRY, FOR POINT ELEMENTS.

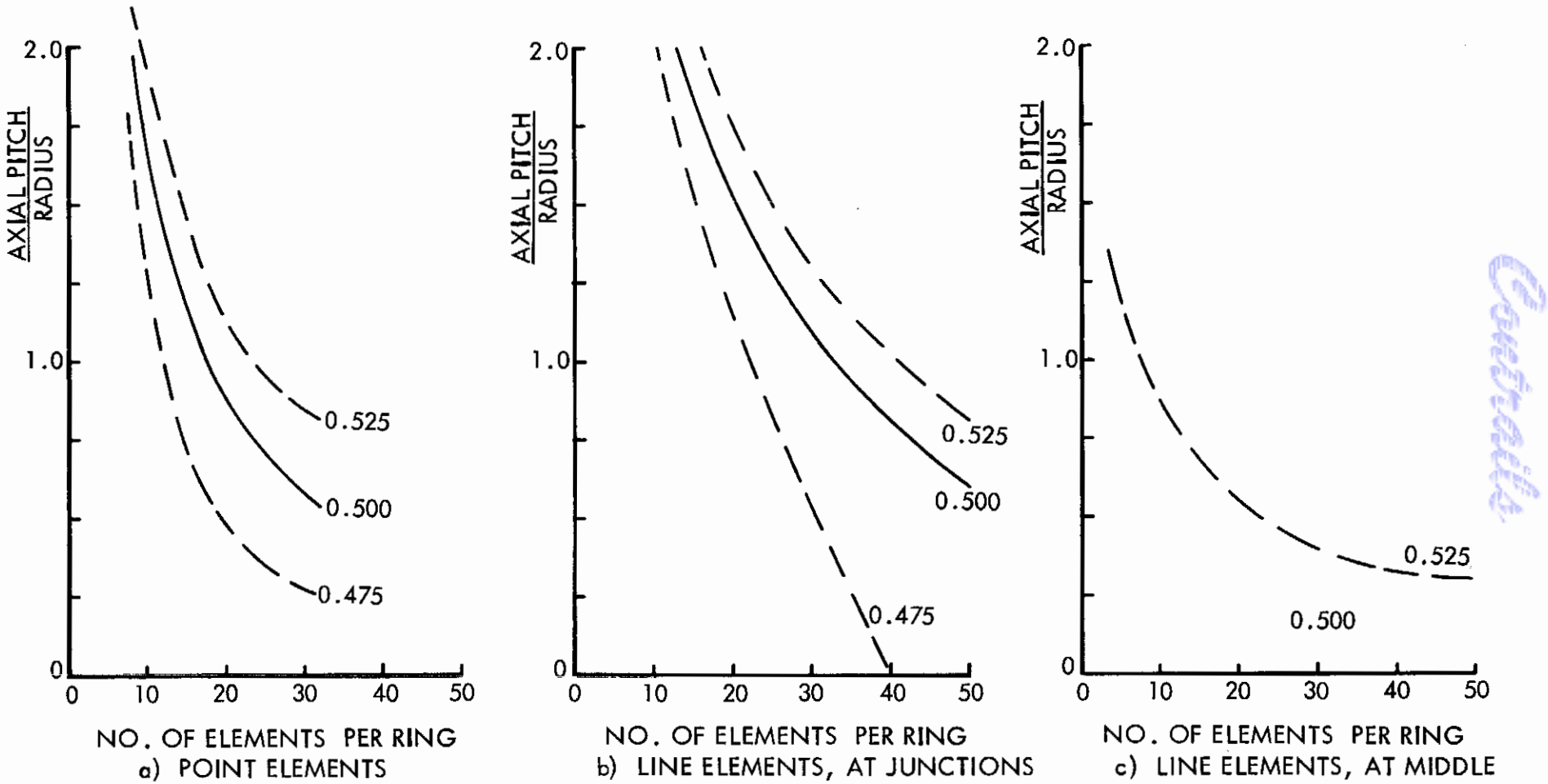

FIGURE 8 ELEMENT GEOMETRIES FOR CORRECT RING-CYLINDER CONVECTION SPEED

SECTION III

COMPUTER PROGRAM DESCRIPTION

1. PROGRAMMING FEATURES

A component programming philosophy was used during the development of the vortex modeling technique. The main program (Version JETP15) provides a framework in which various subroutines can be inserted either to change a particular computational method or to replace a previous routine with an improved one. This approach has proved to be efficient and desirable because of the evolutionary nature of both the aerodynamic and numerical aspects of this modeling technique.

The initial geometry of the vortex modeling network is illustrated in Figure 9. The flow model is composed of a moving vortex-system of short vortex elements, each having three components of a ring vortex element strength simulating the jet flow, and three components of a trailer vortex element strength simulating the crossflow. The resultant component circulation strengths for each short element (CX, CY, CZ) are the algebraic summation of the coincident ring and trailer components, respectively:

$$CX(N) = CXR(N) + CXT(N)$$

$$CY(N) = CYR(N) + CYT(N)$$

$$CZ(N) = CZR(N) + CZT(N)$$

The integrity of the ring and trailer components is maintained throughout the computation, as they are at times used separately. In addition, there is a system of fixed, short, vortex elements representing the "hard surfaces" of the duct and exit plane.

Some important features of the modeling technique are:

- "Short-element" representation of vortex lines
- Simulation of the continuity of vortex lines
- Consideration of the strain of short vortex elements
- Use of a predictor-corrector displacement computation for the jet-plume perturbation procedure
- Simulation of a constant length of jet-plume by a ring injection and throw-away procedure
- Interactive fixed and moving vortex systems in the perturbation procedure
- An analysis of the numerical error/stability during the perturbation procedure
- A collocation point procedure which satisfies the boundary conditions of the duct and exit plane "hard surfaces"
- Explicit computations of the inviscid velocity and pressure distributions on the exit plane.

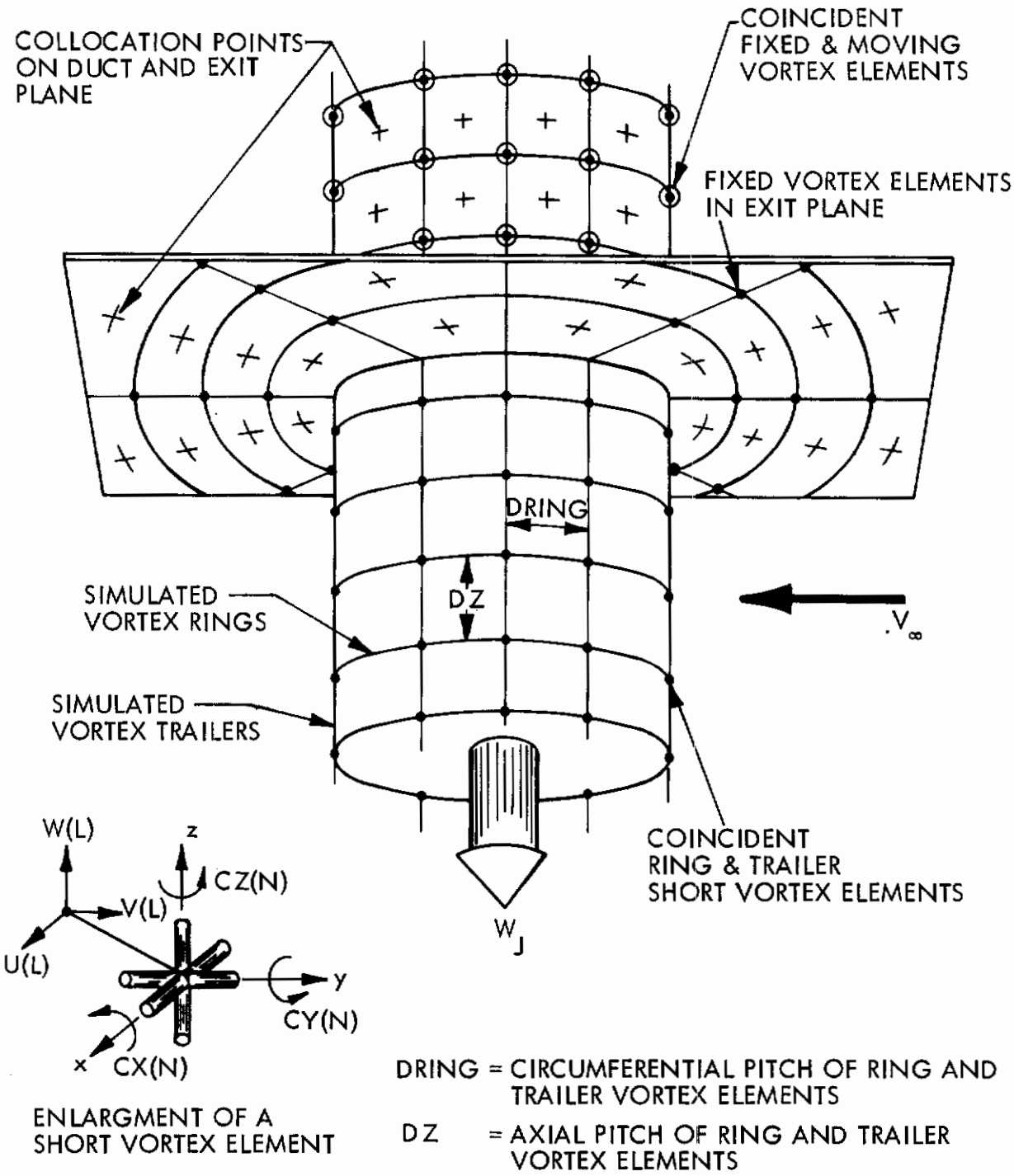

FIGURE 9 ILLUSTRATION OF VORTEX MODELING SYSTEM

The reader is referred to the basic flow chart of JETP15, shown in Figure 10, as a guide to the following discussion of the computer programs' essential operating characteristics. A brief description of various subroutine versions is given in Table I.

2. INITIALIZATION

a. Input Variables

The input variables to the program are described in the first block of the flow chart. Except for the crossflow and jet velocities, the input data pertain to the geometry and perturbation parameters of the vortex systems. The scale of the problem can be specified by the values given to the jet velocity WJ, and the orifice radius, R. For simplicity, these are usually set equal to unity with other parameters normalized accordingly.

b. Initial Conditions

The program first sets up an initial coordinate system for the moving vortex system. The initial spacing given to the ring vortices is so prescribed to give the theoretical ratio of ring self-convection to jet velocity of 0.5. This ring vortex strength then remains constant for the remainder of the run. The initial circulation strength given to the trailer components is somewhat arbitrary; we are using the theoretical value for flow normal to a circular cylinder as a starting condition. Subprogram INCØ10 accomplishes the above setup for the case of a circular cylinder that can be initially titled below the jet exit in the direction of the crossflow and in proportion to the ratio of crossflow-to-jet velocities. Subprogram WRITI prints out the initial conditions of the run.

The initial coordinate system for the fixed-vortex system representing "hard surfaces" is then determined. The fixed-vortex system of the duct is initially coincident with the moving-vortex system of the plume above the exit plane. During the perturbation procedure, the moving system slides along adjacent to this fixed system. Subprogram CPTD1 determines the coordinates of the duct-unit-valued fixed-vortex system and the corresponding coordinates of the collocation points located at the center of the simulated quadrilateral vortices formed by the vortex-element lattice. Subprogram CPTD2 is a similar routine that sets up a standard system for the duct, which may not be initially coincident with the moving system of the jet. (Its optional use will become clearer later on in the discussion.) Subprogram CPTE1 sets up the geometry of the fixed-vortex system representing the exit plane and specifies the coordinates of the collocation points located at the center of the simulated exit-plane quadrilateral vortices. The exit-plane area represented is arbitrary. We currently have a circular area with a radius of 6R centered at the jet orifice.

3. PERTURBATION PROCEDURES

a. Forward Perturbation Loop

The first step in the perturbation procedure is to compute the induced velocity at each moving-element location due to all the other moving-vortex elements. In addition, the induced effect of the fixed vortex system on the moving elements that are below the exit plane is computed. The basic equation for these computations is the Biot-Savart law adapted to the short-element concept. By considering the enlargement of a short vortex element illustrated in Figure 9, these equations for the induced velocity components at an element location (L) have the form:

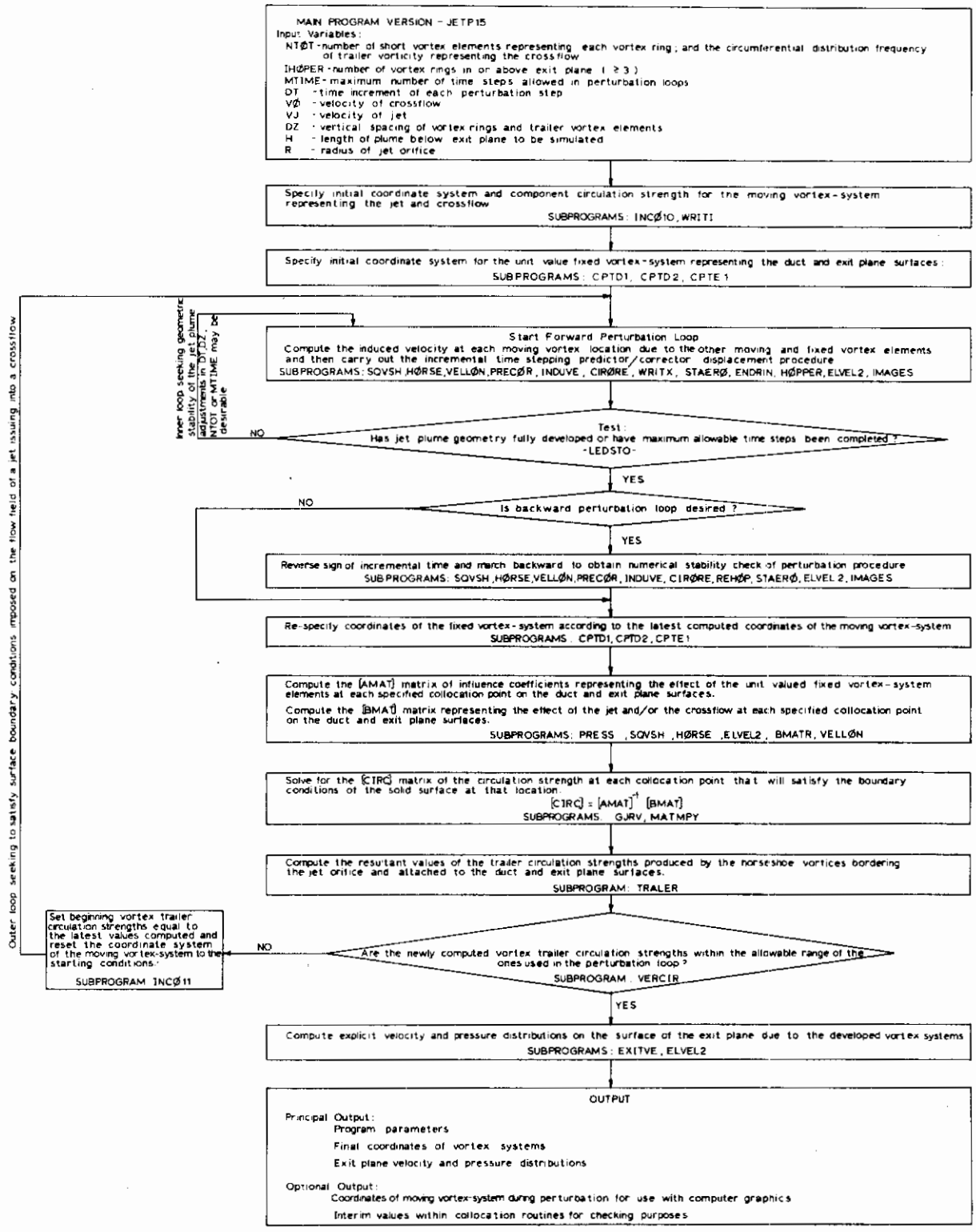

FIGURE 10 BASIC FLOW CHART FOR VORTEX MODELING OF A JET IN A CROSSFLOW

TABLE I

DESCRIPTION OF PROGRAM SUBROUTINES

Subroutine/Versions	Description
WRITI/WRIT11	Output of program parameters and initial coordinates and circulation strengths of the moving-vortex system.
WRITX	Output of coordinates of moving-vortex system during perturbation loop.
INICØR/INCØ10	Setup of initial moving-vortex system coordinates and component circulation strength.
/INCØ11	Setup of moving-vortex system based on results of collocation procedure for surface boundary conditions.
PRECØR/PRECØ1	Predictor/corrector perturbation procedure for moving-vortex system.
/PRECØ2	Predictor/corrector perturbation procedure with interactive fixed and moving-vortex systems.
ELEVEL	Short element induced velocity computation for dimensioned input.
ELEVEL2	Short element induced velocity computation for non-dimensioned input.
VELLON	Long element induced velocity computation.
IMAGE	Coordinate imaging for symmetrical geometry.
STAERØ/STAERS	Statistical analysis of cumulative numerical error in perturbation program.
HØPPER/HØPP10	Simulates constant length of plume during forward marching in perturbation program.
REHØP/REHØ10	Simulates constant length of plume during backward marching in perturbation program when optional numerical error analysis is being performed.
ENDRIN/ENDRI0	Saves discarded end ring of moving-vortex system for use with REHØP.
CIRØRE/CIRØR1	Orientates circulation vector during each perturbation step to preserve continuity of vortex lines.
/CIRØR2	Same as above but includes the effects of vortex element strain on the component circulation strengths.

TABLE I (Continued)

DESCRIPTION OF PROGRAM SUBROUTINES

Subroutine/Versions	Description
LEDSTØ/LEDST1	Geometric convergence criteria based on four leading-edge elements of jet plume.
/LEDST2	Geometric convergence criteria based on least-squares fit of jet plume path.
PRESS/PRESS3	Collocation procedure for satisfying pressure convergence criteria imposed by the duct and exit plane boundary conditions; used when PRECØ1 is specified.
/PRESS4	Similar to above but structured for use when PRECØ2 is specified.
INDUVE	Induced velocity routine used in conjunction with PRECØ2 which includes the effects of the moving- and fixed-vortex systems in the perturbation loop.
CPTD1	Sets up the variable-geometry fixed-vortex and collocation-point systems for the duct.
CPTD2	Sets up constant geometry fixed-vortex and collocation-point systems for the duct.
CPTE1	Sets up constant geometry fixed-vortex and collocation-point systems for the exit plane.
SQVSH/SQVSH4	Calculates velocity at arbitrary point induced by short elements simulating long element quadrilateral vortex.
/SQVSHL	Calculates velocity at arbitrary point induced by long element quadrilateral vortex.
HORSE/HORSE2	Calculates velocities at an arbitrary point induced by all the short vortex element trailers extending below the exit plane. These trailers are the downstream extensions of horseshoe vortices which are on the duct and exit plane surfaces and adjacent to the jet orifice.
/HORSEL	Similar to above but structured for long element computation.
BMATR/BMATR4	Calculates the induced effect on the collocation points of the moving ring vortices and freestream velocity below the exit plane.
/BMATR5	Calculates the induced effect on all collocation points of only the freestream velocity below the exit plane.
TRALER	Calculates the resultant circulation strength at each trailer location extending from the jet orifice.

TABLE I (Concluded)

DESCRIPTION OF PROGRAM SUBROUTINES

Subroutine/Versions	Description
VERCIR	Compares the previous trailer circulation strengths with the new values obtained from the collocation procedure and replaces them if agreement criteria is not satisfied.
EXITVE	Calculates explicit exit plane velocity and pressure distributions based on the final circulation strengths of the fixed- and moving-vortex systems simulating the jet plume in a crossflow.
SQVSHC	Calculates velocity at an arbitrary point induced by the resultant circulation strength of the short element quadrilateral vortice about each collocation point.

$$U(L) = (1/4\pi R_L^3) \sum_{N=1}^{N_M} \{CZ(N) \cdot (Y(N)-Y(L)) - CY(N) \cdot (Z(N)-(ZL))\}$$

$$V(L) = (1/4\pi R_L^3) \sum_{N=1}^{N_M} \{CX(N) \cdot (Z(N)-Z(L)) - CZ(N) \cdot (X(N)-X(L))\}$$

$$W(L) = (1/4\pi R_L^3) \sum_{N=1}^{N_M} \{CY(N) \cdot (X(N)-X(L)) - CX(N) \cdot (Y(N)-Y(L))\}$$

where N_M is the total number of vortex elements acting on the element (L), and R_L is the distance between points N and L.

Subroutine PRECØR provides the computational framework for determining the induced velocities and computing the incremental displacements of the moving-vortex elements during the development of the plume flow field. An important aspect of this perturbation procedure in terms of accuracy and computer efficient is the use of a predictor-corrector computation for the element displacements. A more detailed description of this technique is contained in Section V, 1.b.

After each time step, the circulation vector of each moving vortex element is reoriented to a direction consistent with the Helmholtz requirement for the continuity of vortex lines. Also, if the length of vortex line represented by each short element has changed, the circulation strength of that element is adjusted to accommodate the strain experienced. Subroutine version CIRØRE/CIRØR2 performs these computations. Subroutine WRITX reads out the coordinates of the moving-vortex system at specified time-step intervals. These data can then be visually analyzed with computer-graphics techniques.

If precautions were not taken during the forward marching, the whole moving-vortex system would be convected downstream analogous to actual fluid flow. To simulate a constant length of plume (i.e., a constant number of vortex elements) in a stationary coordinate system, requires the addition and removal of vortex elements at appropriate intervals. Subroutine HØPPER does this by monitoring the convection of the top ring of the jet. When this ring has traveled one axial pitch (DZ) in the jet direction, a new vortex ring of equal circulation value is inserted above it, and the vortex ring at the bottom of the plume is removed and saved by Subroutine ENDRIN for later use if backward marching is specified. The physical effect of this hopper process is analogous to the location of a fan at the ring injection point, as has been discussed in Section II.

The forward marching is allowed to proceed until the plume geometry has reached a stable configuration, or the maximum number of time-steps have been completed. Plume-stability criteria might be satisfied, for instance, by no further movement of the plume leading edge. Subroutine version LEDSTØ/LEDST2 fits a three-degree polynomial through these points and compares the relative motion of this curve from one time step to another. Although this method has been used successfully, another approach is usually employed which is not as sensitive to plume irregularities. This is to allow a maximum number of time steps to take place such that the plume appears to have developed fully. This can be based on experience and observations using computer graphics. Either approach can be implemented with only a few FORTRAN statement changes.

b. Backward Perturbation Loop

When the forward perturbation loop is terminated, an option is available for reversing the perturbation procedure by changing the sign of DT and marching backward. Subroutine REHØP tracks this motion, replaces the appropriate saved end-ring at the bottom of the plume, and takes a top ring off at the same time step as the reverse was done during the forward marching. Cumulative numerical error terms can be computed by comparing the differences between the vortex system coordinates at a particular time step. Subroutine STAERØ performs a statistical analysis of these numerical errors. However, since the backward marching about doubles the computer time of the run, this error analysis is performed only when there is particular need. Results of a study of the parameters affecting the magnitude of the numerical error in the perturbation procedure are presented in Section V. Guidelines have been established which usually can alleviate the numerical stability problem to a great extent.

4. COLLOCATION PROCEDURE FOR "HARD" SURFACES

When the perturbation loop is completed, the coordinates of the fixed-vortex system are adjusted so as to reflect the new location of the intersection of trailer vortex lines and the exit lip of the jet orifice. This is necessary, since the exit plane vortex elements are located along rays extending outward from these intersection points. The net effect of this adjustment is a slight relaxation of the fixed vortex system in the direction of the crossflow. Subroutines CPTD1, CPTD2, and CPTE1 are called again for this purpose.

There are several possibilities for establishing the simulated horseshoe vortices at the jet orifice, depending on the relative position of a ring element intersecting the exit plane. Figure 11 illustrates the case where the center of the last quadrilateral vortex partially on the duct is below the exit plane. Since collocation points must be on "hard" surfaces, the horseshoe vortex is extended up around the collocation point directly above. This somewhat random formulation of the duct horshoe vortices, accomplished with Subroutine CPTD1, could cause time-dependent fluctuations in the collocation results. If this is the case, Subroutine CPRD2 can be used as an optional approach to establish a standard collocation point system for the duct using the same lip intersection points determined in CPTD1.

Subroutine PRESS4 provides the overall framework for the collocation procedure. The first step is to calculate an influence coefficient matrix (AMAT) for the unit-value fixed-vortex system at each collocation point specified on the duct and exit-plane surfaces. Subroutine SQVSH4 is called to calculate the velocity at each collocation point induced by each simulated long-element quadrilateral formed by the short-vortex elements of the fixed-vortex system. Subroutine HØRSE2 computes the velocity at each collocation point induced by the system of vortex-element trailers extending below the exit plane. For near-field computations, actual vortex lines as opposed to short elements may be necessary for improved accuracy. Subroutine versions SQVSHL and HORSEL are available for this purpose. The AMAT matrix is then computed as

$$\left[AMAT(N,L)\right] = \sum_{N=1}^{IXXT} \sum_{L=1}^{IXXT} \left[U(L) * \varphi_1(N) + V(L) * \varphi_2(N) + W(L) * \varphi_3(N)\right]$$

where U, V, and W are the velocity components at collocation point (N) induced by quadrilateral or horseshoe vortex; and φ_1, and φ_2, and φ_3 are the direction cosines for

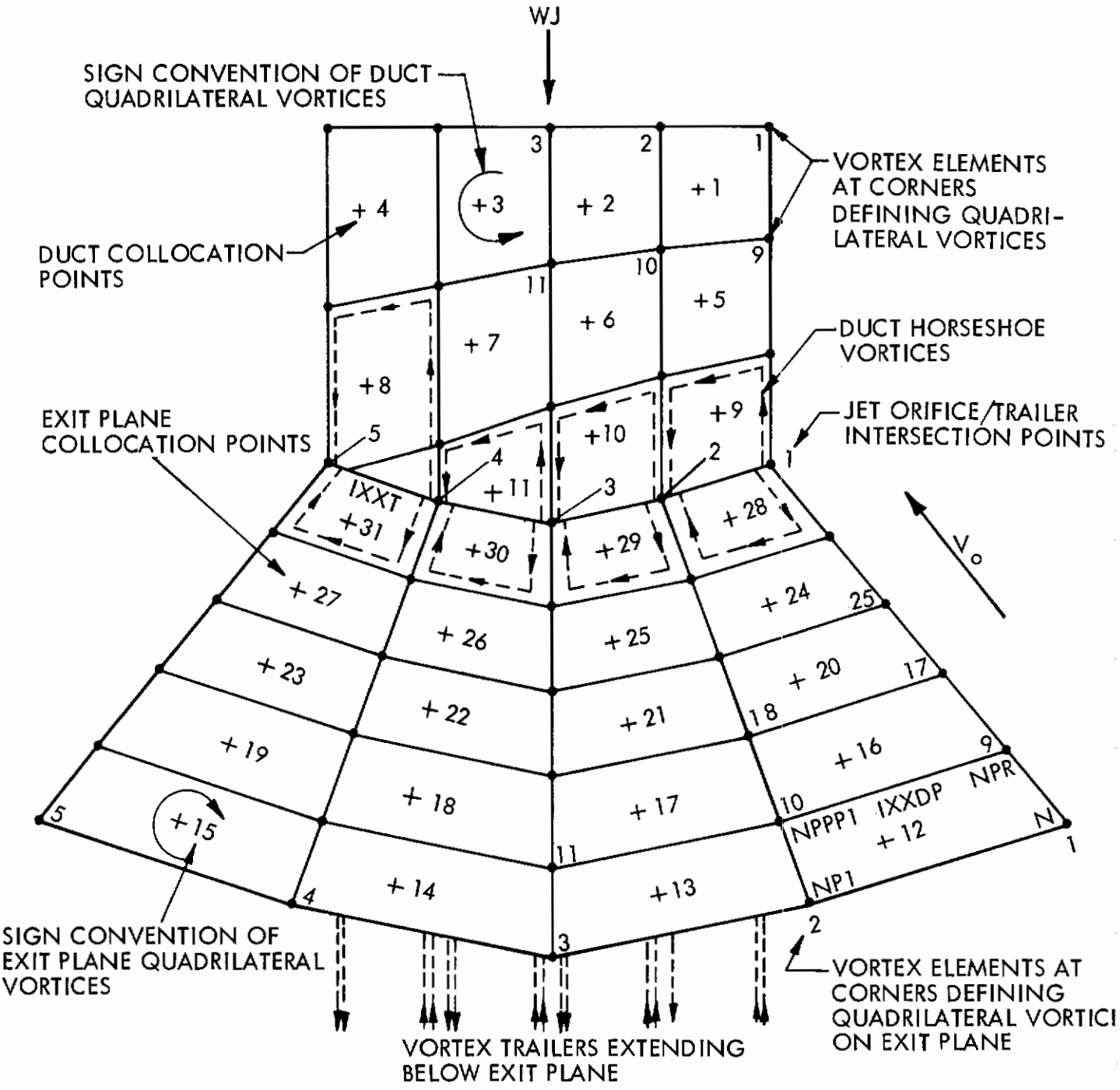

FIGURE 11. FOLDOUT HALF-VIEW OF FIXED VORTEX-SYSTEM & COLLOCATION POINTS REPRESENTING THE DUCT & EXIT PLANE SURFACES

tangential flow at the collocation point (N). IXXT is the total number of collocation points.

A matrix of the induced velocity at each collocation point resulting from the ring elements of the moving vortex-system and/or the effect of the crossflow on each collocation point is computed by Subroutine BMATR. The following matrix equation is then solved for the unknown circulation values at each collocation point which satisfies the "hard surface" boundary conditions:

$$[\text{CIRC}][\text{AMAT}] = [\text{BMAT}]$$

Subroutines GJRV and MATMPY are, respectively, a Gauss-Jordan matrix inversion program and a matrix multiplication program.

The circulation values of the horseshoe vortices on the duct and exit surfaces that border the jet orifice are then combined appropriately by Subroutine TRALER to yield new values for the trailer vortex of the moving system. These new values are compared with the ones used during the perturbation loop by Subroutine VERCIR. If they are significantly different (e.g., an average deviation for all trailer circulation values, say, greater than 10%), the new trailer values are used in the initialization procedure of Subroutine INCØ11, and the perturbation loop is invoked again.

Once the trailer vortex values have converged, then Subroutine EXITVE is called to compute the inviscid exit-plane velocity and pressure distributions resulting from the modeled flow field.

SECTION IV

COMPUTER GRAPHICS

Although computer graphics is not an implicit part of the solution of the jet-plume problem, it proved to be an almost essential tool for program development, particularly for checking out perturbation programs. The various computers used are listed in Table II, together with the tasks for which we used them. As the UNIVAC 418 graphics computer was too slow for the main calculations, paper tape or cards were carried to it from the faster machines. On numerous occasions, the combination of good graphical display of the results, together with our aerodynamic knowledge, made the diagnosis of program errors possible much more quickly than by alternative means. This point may be emphasized by reference to the number of points contained in Figure 1, for example, which is just one frame of a time-varying sequence.*

The computer-graphics program reads a sequence of definitions of complete plume geometries from paper tape or cards and constructs a time history of this evolution. During display, motion may be stopped by using an interrupt switch, and the "object" may be rotated continuously to a more favorable view, before continuing with the time history. Although the rotational motion, particularly, lends a three-dimensional effect, dimming of distant lines is also used to this end. In another mode, it is possible to illuminate strongly only one ring and to watch its progress down the plume.

TABLE II

DESCRIPTION AND TASK OF COMPUTERS USED

Computer	Description and Task
'RAX'	Remote terminal to IBM 360-50, 14k storage of 14-bit words, 10-minute limit on execution time. Paper-tape and teletype output. Used for program check-out and small runs. Situated at Aerospace Research Laboratory.
UNIVAC 418	Has extensive graphics capability, including interactive mode. Used as display device for output from either "RAX" or one of the larger computers.
CDC 6400	64k storage, 32-bit words, card output. Used as our main computer, for batch work, before its removal in mid-1970.
UNIVAC 1108	Similar general capability, for our purposes, except for 16-bit words. Used for batch work after removal of CDC 6400.

*The authors greatly appreciate the timely and skilful help given by David M. Smith, of the Lockheed-Georgia Systems Sciences Laboratory, who developed the computer graphics software for this project.

SECTION V

NUMERICAL ACCURACY AND STABILITY CONSIDERATIONS

1. VORTEX-ELEMENT DISPLACEMENT

a. Comparison of Time-Stepping Methods

The actual path of a vortex element during flow modeling is a function of the displacement method and the size of the time increment used in the time-stepping procedure. The calculated path is only an approximation because the mutually induced velocity field computed to determine each incremental displacement is accurate only for one instant in time. Therefore, the larger the time step, the greater will be the error of the small displacement. However, even for the same time increment, the formulation of the displacement equation can greatly affect the magnitude of error. In Reference 7, a comparison was made among the Euler Method (using the first two terms of a Taylor expansion series), a second-order Runge-Kutta Method of extrapolating in time, and a one-step predictor-corrector method. The latter method (described in the following paragraph) is by far the superior of the three, as indicated by the results shown in Figure 12, and it has been used exclusively for the three-dimensional modeling program.

b. Predictor-Corrector Method

The predictor-corrector method is a one-step, second-order, computation in which the desired element displacement is defined as the midpoint of the resultant of two Euler-method vectors $U_i(t) \cdot Dt$ and $U_i(t+Dt) \cdot Dt$, as illustrated in the sketch below:

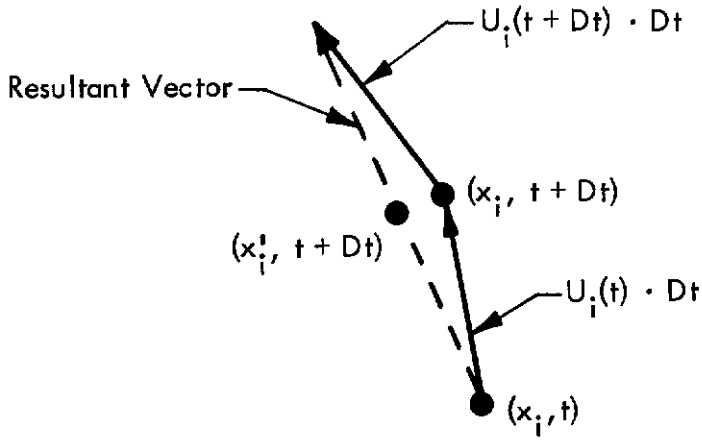

Vortex Element in
the Velocity Field U_i

U(t) is the initial value of the induced velocity field due to the vortex elements in the system, and U(t + Dt) is the value of this field based on the relative position of these vortex elements at time (t + Dt). The general equation for the predictor-corrector method is easily shown to be:

$$x_i'(t + Dt) = \frac{1}{2} \{x_i(t) + x_i(t + Dt) + U_i(t + Dt) \cdot Dt\}$$

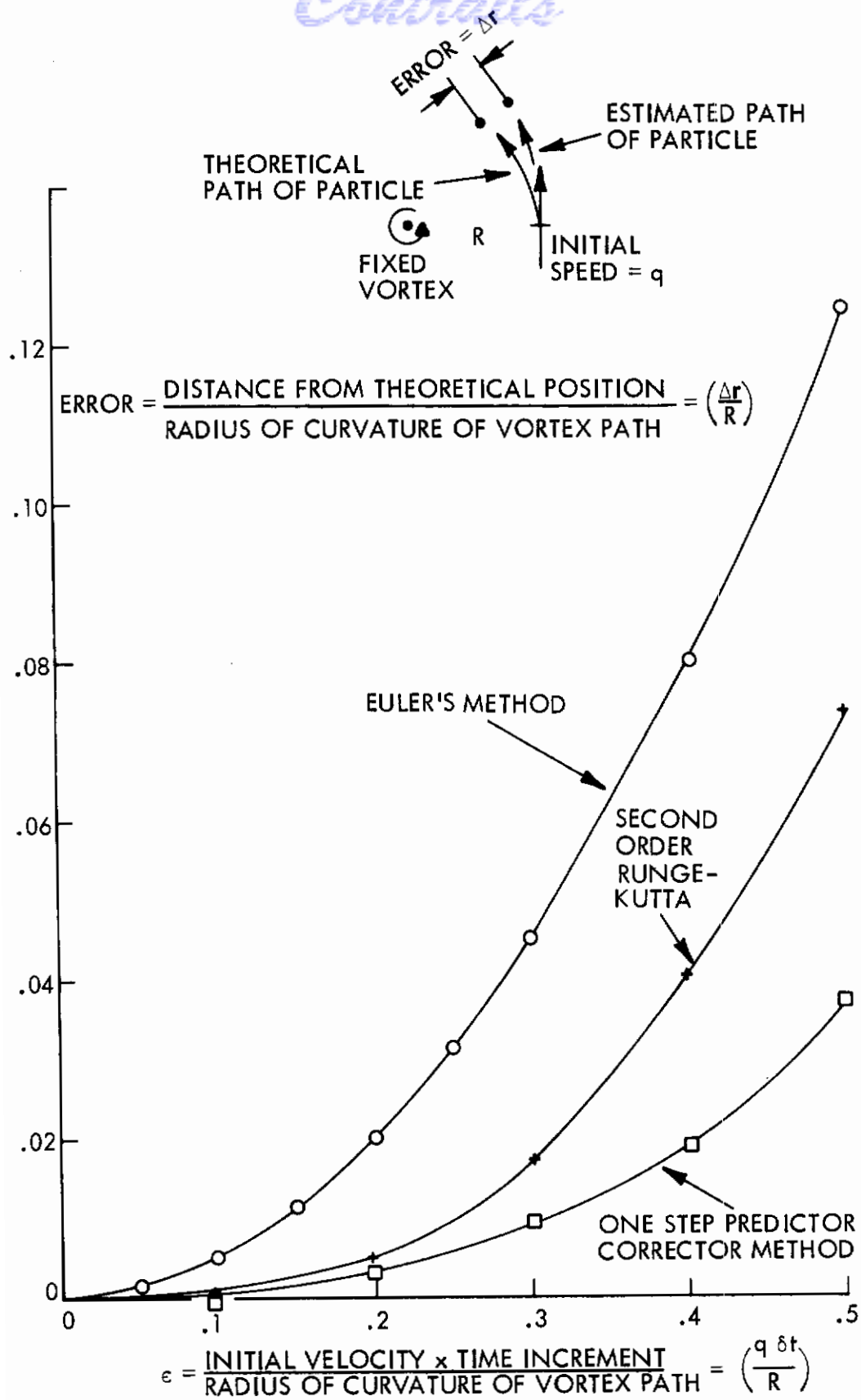

FIGURE 12 ERROR IN ESTIMATING THE VORTEX MOVEMENT IN SPACE FOR SEVERAL METHODS OF TIME-STEPPING

where i = 1, 2 or 3, for the respective x, y, or z componens of the three-dimensional field.

2. CUMULATIVE ERROR OF MOVING-VORTEX SYSTEM

a. Statistical Error Parameters

The previous subsection dealt with the displacement error of a vortex element during a single time step. In the modeling technique, there is a moving-vortex system containing many vortex elements which are allowed to move about for a sufficient number of time steps to form a rolled-up plume geometry. If the cumulative numerical error becomes too large, the vortex systems will be unstable, and a good simulation of the real flow will not be achieved.

An obvious way to assess the accuracy and stability of the perturbation procedure is to compare the vortex-system coordinates at some point in time, while marching forward, with the coordinates obtained for the same point in time after reversing the sign of Dt and marching backward. The sketch below illustrates the distortion that might occur as a result of the cumulative numerical error:

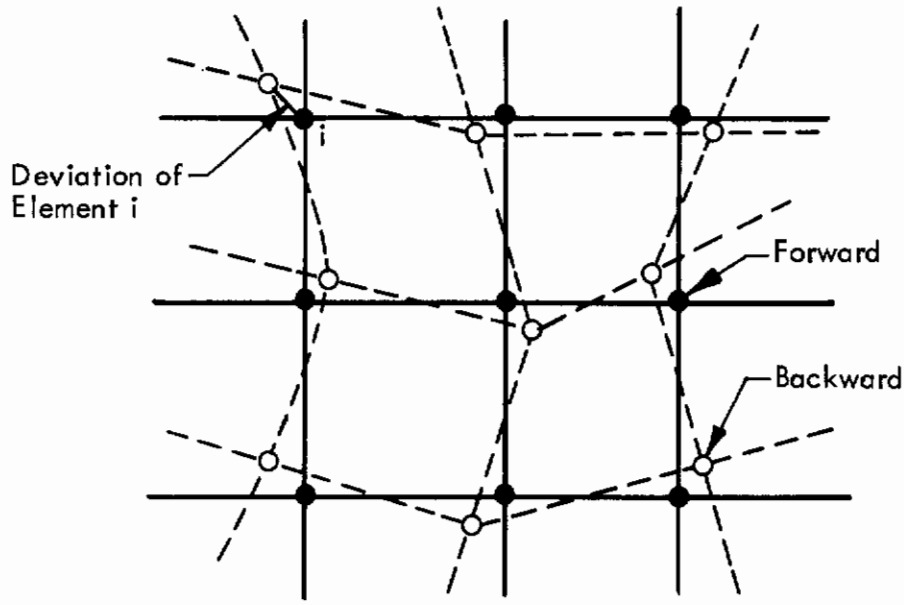

The deviation magnitude (d_i) for each vortex element can be defined relative to the jet orifice radius (R) as

$$d_i = \frac{\left[(\Delta x)^2 + (\Delta y)^2 + (\Delta z)^2\right]^{1/2}}{R}$$

and can be thought of as a random variable of the complete vortex system. Therefore, we can use statistical terms to describe the apparent degree of error or stability. For instance, the arithmetic mean, defined as

$$\text{Arithmetic Mean} = \frac{1}{N_M} \sum_{i=1}^{N_M} d_i$$

where N_M is the total number of elements in the system, could be a measure of local instabilities, since a few elements with large deviations would cause this value to be large even though most of the deviations may be quite small. On the other hand, the geometric mean, defined as

$$\text{Geometric Mean} = (d_1 \cdot d_2 \cdot d_3 \ldots . d_N)^{1/N}$$

is more of a measure of the overall cumulative error, since it indicates the most typical (or frequent) size of each deviation in the population.

The following subsections present the results of statistical studies of various modeling parameters on the accuracy and stability of the perturbation procedure.

b. Effect of Computation Parameters

The trends shown in Figure 13 illustrate the sensitivity of the geometric mean deviation to several nondimensionalized modeling parameters. A geometric mean of 10^{-1} or less is thought to be an acceptable level in most computations, since this represents a cumulative error of 10 percent or less of R for both forward and backward marching. As expected, the time-step size parameter (WJ · Dt/DZ) has a significant effect. The ratio of the axial to circumferential pitch (DZ/DRING) of the vortex element is also important, particularly when the crossflow-to-jet velocity ratio (VO/WJ) is greater than zero. The interesting result shown in the figure is that, for most cases, the geometric mean deviation decreases with decreasing time-step size parameter, while the total time of the perturbation procedure remains constant. However, to keep the total time constant as Dt decreases requires more time steps and a correspondingly longer computer run time.

c. Effect of Short-Element Constraints

It has been noted previously that, to satisfy certain theoretical constraints, the short-element circulation vector should be consistent with the strength and direction of the vortex line segment represented. The data for VO/WJ= 0.2 and N_R = 8, shown in Figure 14, indicate a reduction in accuracy by applying first the vector-orientation constraint and then the vector-strength constraint to the perturbation procedure. That is, for the latter case, both the direction and strength of each short-vortex element is recomputed after each time step. Further studies have shown that this destabilizing trend is proportioned to the number of elements per ring (N_R).

d. Effect of Computer Precision

An example of the relative effect of word length on the accuracy of the perturbation technique is illustrated below for the case where

$$N_R = 8,\ R = 1.0,\ H_P = 6.0,\ T_M = 10$$

$$WJ \cdot DT/DZ = 1.0,\ VO/WJ = 0.2,\ DZ/DRING = 1.273$$

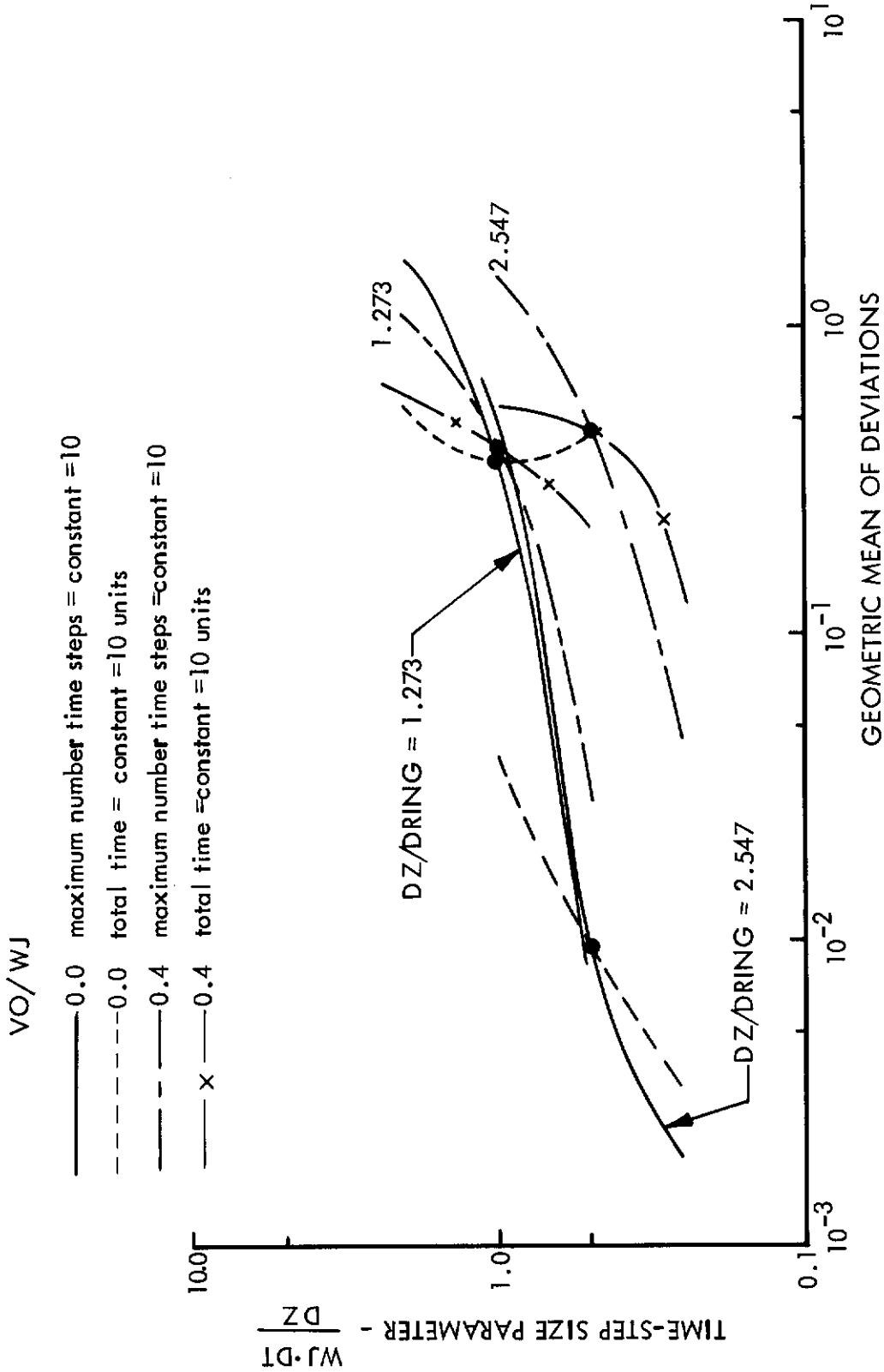

FIGURE 13. EFFECT OF COMPUTATIONAL PARAMETERS ON NUMERICAL ERRORS.

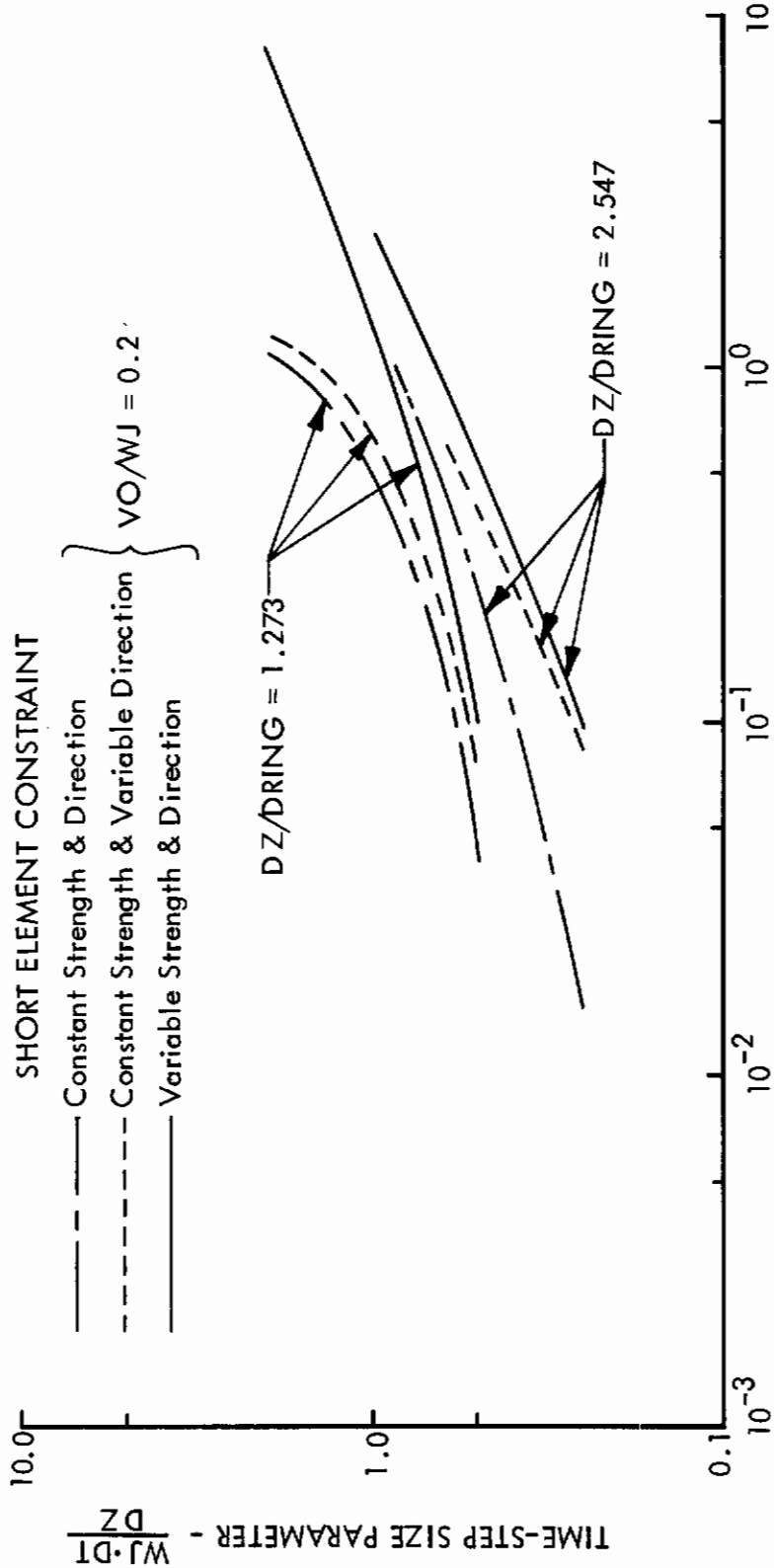

FIGURE 14. EFFECT OF SHORT ELEMENT CONSTRAINTS ON NUMERICAL ERRORS.

Deviation Statistics	16 Bit Word Length	32 Bit Word Length
Geometric Mean	9.390×10^{-2}	7.951×10^{-2}
Arithmetic Mean	1.265×10^{-1}	1.107×10^{-1}
Standard Deviation	9.914×10^{-2}	7.457×10^{-2}

These results indicate that there is little incentive to specify a 32-bit word length if this requires double-precision arithmetic.

SECTION VI

MODELING RESULTS FOR A JET IN CROSSFLOW

1. IMPLEMENTATION OF THE MODELING TECHNIQUE

The object of this research is to develop a numerical method of modeling the interaction of a jet issuing normal to a subsonic crossflow, and to determine the interference pressure field produced on surfaces near the jet exit. The current results are intended to confirm the validity of this modeling concept and to demonstrate the computer program that has been developed. The preliminary contours presented are not intended for comparison with experimental measurements, since additional refinements, including viscous effects, more sophisticated vortex-element types, and better integration schemes, are desirable for better physical representation and computation efficiency.

2. BOUNDARY-CONDITION CONVERGENCE

A principal feature of the modeling method is independence from empirical input. The plume is allowed to evolve with mutual interaction of the vortex elements. A proper path is achieved by allowing the vortex trailer circulation strengths to be determined by using the flow tangency condition at the wetted surfaces of the duct and on the exit plane. This circulation-convergence process, which essentially effects the distribution of the trailer circulation strengths around the periphery of the jet, normally takes two or three iterations (see Figure 15). Circulation convergence can be achieved at any desired stage of plume development. Transient solutions are possible, if needed, without allowing the plume to reach a final steady state.

3. PLUME GEOMETRIES

For crossflow-to-jet velocity ratios (VO/WJ) of 0.3 or greater, the plume geometry develops a reasonably stable trajectory with a well developed rolled-up vortex system. A time-history sequence for VO/WJ = 0.3, taken from the computer-graphics display scope, is shown in Figure 16. A somewhat disappointing result has been the lack of stability for the lower velocity ratios where the crossflow has a weaker effect. In these cases, the upper portion of the plume tends to billow forward, and the lower portion tends to whip about somewhat like the end of a hose when freed. This is attributed to the sudden removal of ring-circulation strengths at the end of the plume. Typical plume geometries for the range of VO/WJ from 0.1 to 0.4 are shown in Figure 17. There is an evident improvement in geometric stability with increases in velocity ratio.

Several observations can be made concerning the effect of varying starting conditions on the time history of the plume. For example, the photos shown in Figure 18 illustrate a saving in plume development time when the plume has an initial slope in the direction of the flow. Also, if the initial trailer circulation strengths are significantly greater than the potential cylinder values, the plume becomes unstable quite rapidly. This suggests that making the two iteration loops more interactive could improve the development of the less-stable cases. Further study is needed regarding the strategic use of the various parts of the program.

4. EXIT-PLANE VELOCITY AND PRESSURE DISTRIBUTIONS

The principal requirement for the modeling program is to compute the velocity and pressure anywhere in the flow field; the pressure distribution on the exit plane of the jet orifice is particularly important. The interference forces produced by the jet-crossflow interaction may be determined from the pressure distribution. The pressure contours plotted in Figure 19 for VO/WJ = 0.1 and 0.2 illustrate a low-pressure region on the sides of the orifice, which shifts rearwards and intensifies as the velocity ratio increases.

Figure 20 shows pressure contours for VO/WJ = 0.3 halfway through the plume development and after a representative path was achieved. The shift of the low-pressure region to the downstream side of the orifice, as the plume bends with the crossflow and forms the strong rolled-up vortex formation, is quite evident. A very strong negative pressure gradient develops in the region where real flows are known to separate. Of course, the pressure contours beyond this region and downstream of the jet orifice represent only the theoretical inviscid result. The low-pressure bubbles within the lobe are believed to result from local effects of the vortex lattice system in the plume.

Increasing VO/WJ to 0.4 accentuates the downstream shift and intensity of the low-pressure region, as shown by the pressure contour plotted in Figure 21. Here, the plume development was the same as the VO/VJ = 0.3 results shown on the right-hand side of Figure 20. The corresponding velocity field for VO/WJ = 0.4 is also plotted on Figure 21. Again, the closure of the flow downstream of the jet orifice demonstrates the potential-flow nature of the current modeling method.

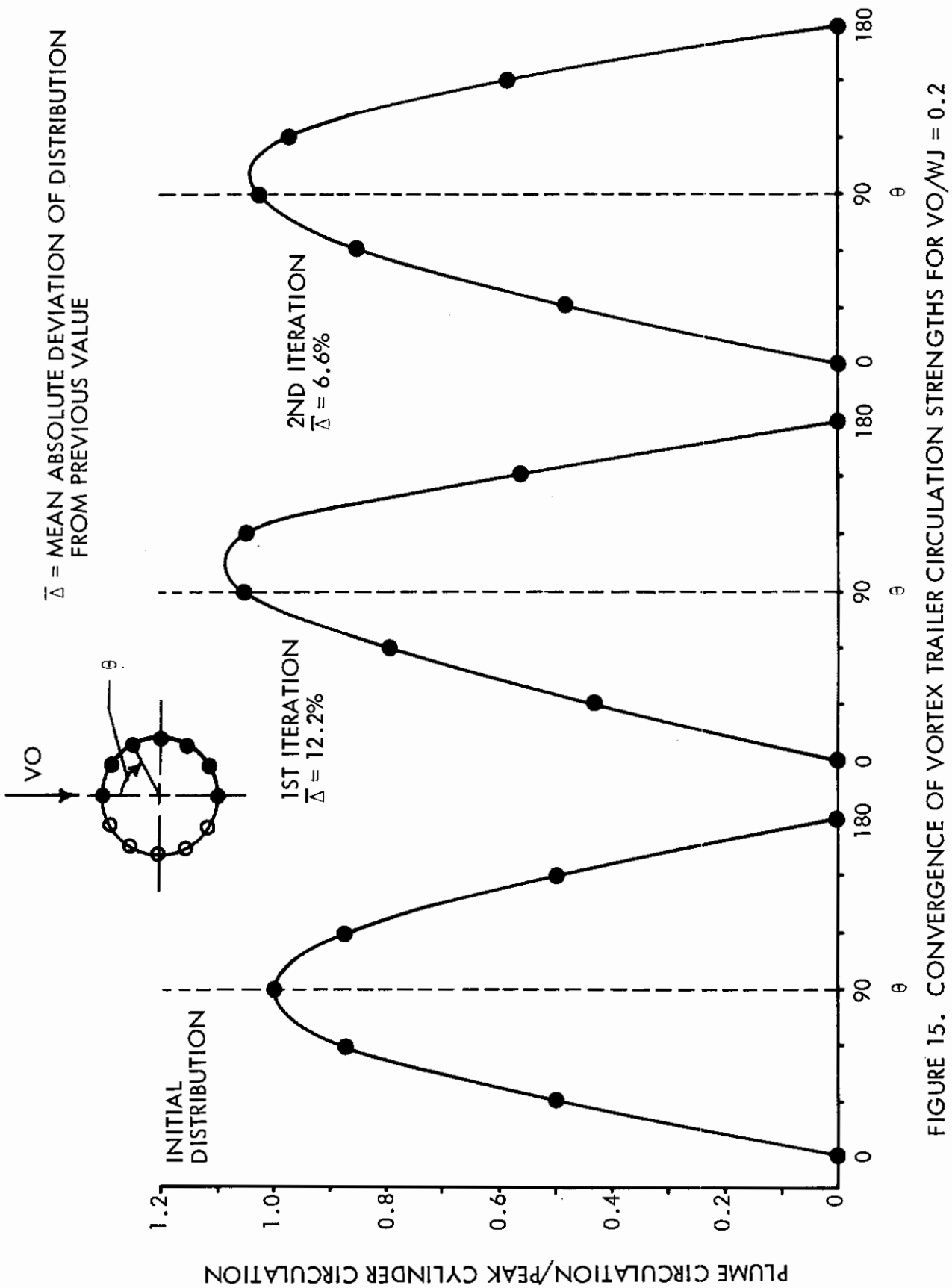

FIGURE 15. CONVERGENCE OF VORTEX TRAILER CIRCULATION STRENGTHS FOR VO/WJ = 0.2

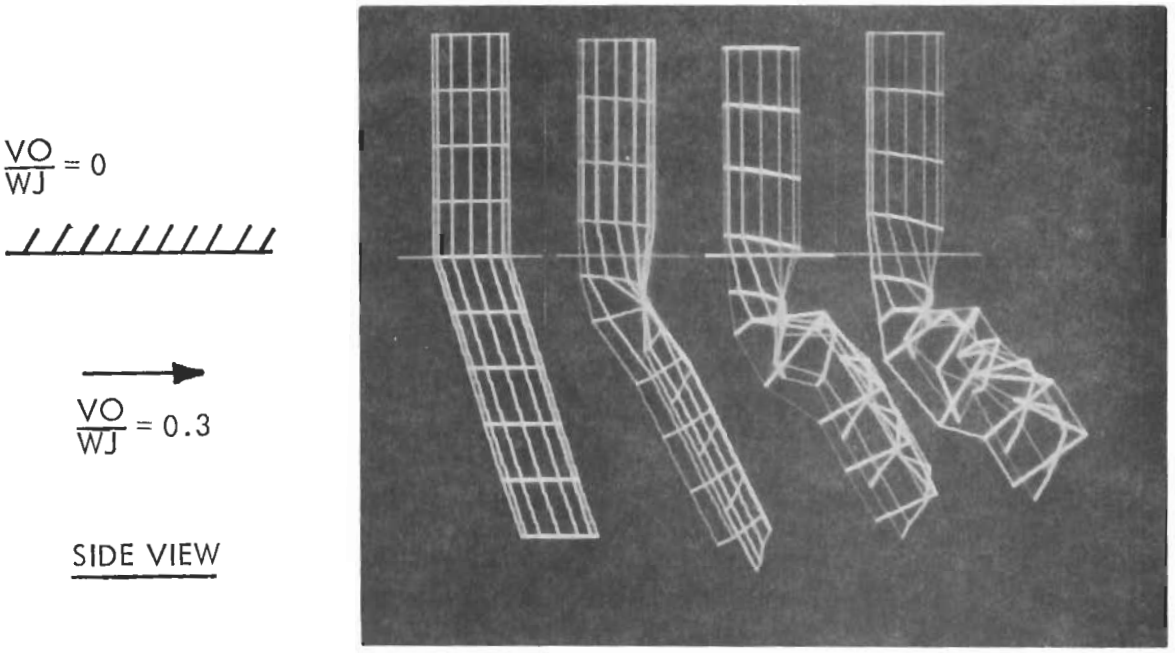

FIGURE 16. TIME HISTORY OF PLUME GEOMETRY

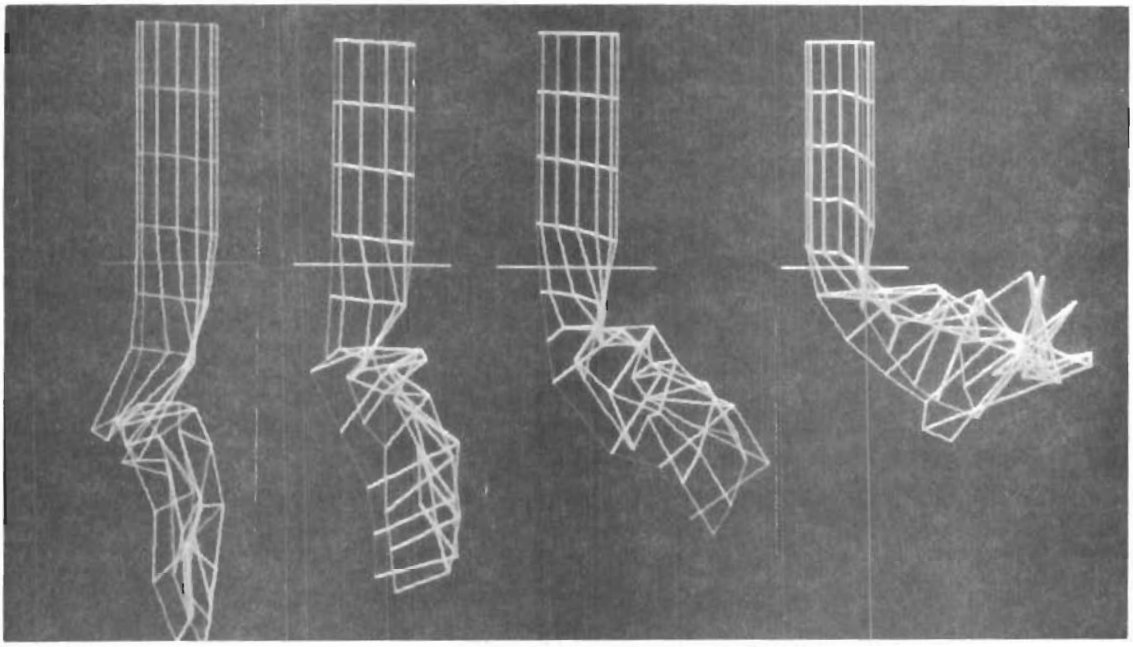

VO/WJ = 0.1 0.2 0.3 0.4

FIGURE 17. PLUME GEOMETRY VS. VO/WJ VELOCITY RATIO

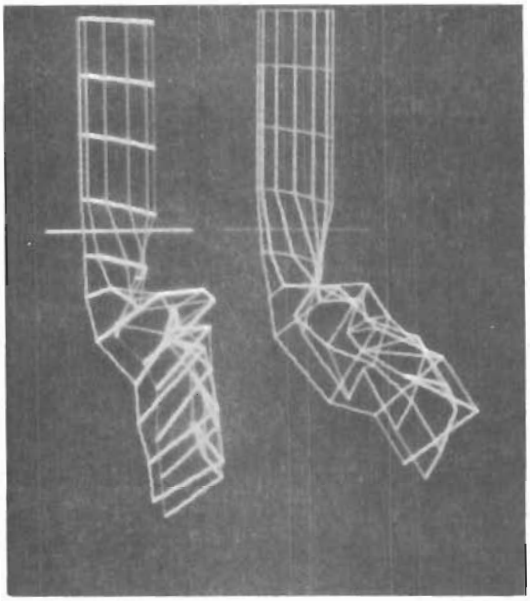

0.0 0.3

(a) INITIAL SLOPE BELOW EXIT

(T·WJ)/R = 12.0

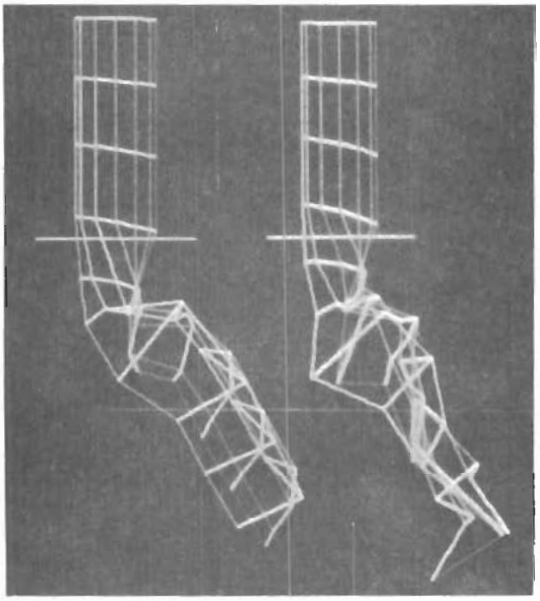

1.0 1.5

(b) PLUME TRAILER CIRCULATION / CYLINDER CIRCULATION

(T·WJ)/R = 9.0

FIGURE 18. EFFECT OF STARTING CONDITIONS ON PLUME DEVELOPMENT

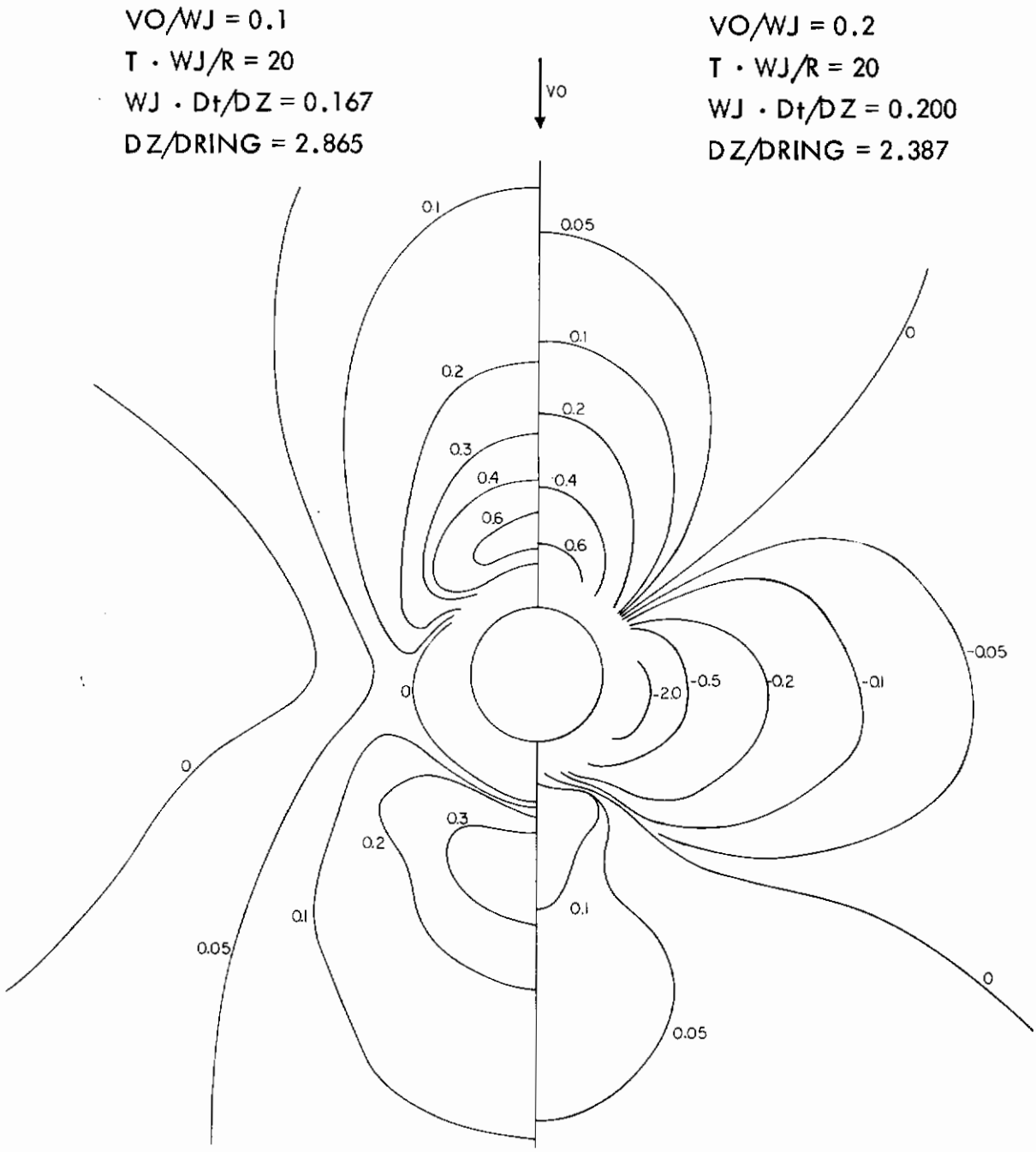

FIGURE 19. PRESSURE DISTRIBUTIONS FOR VO/WJ = 0.1 AND 0.2

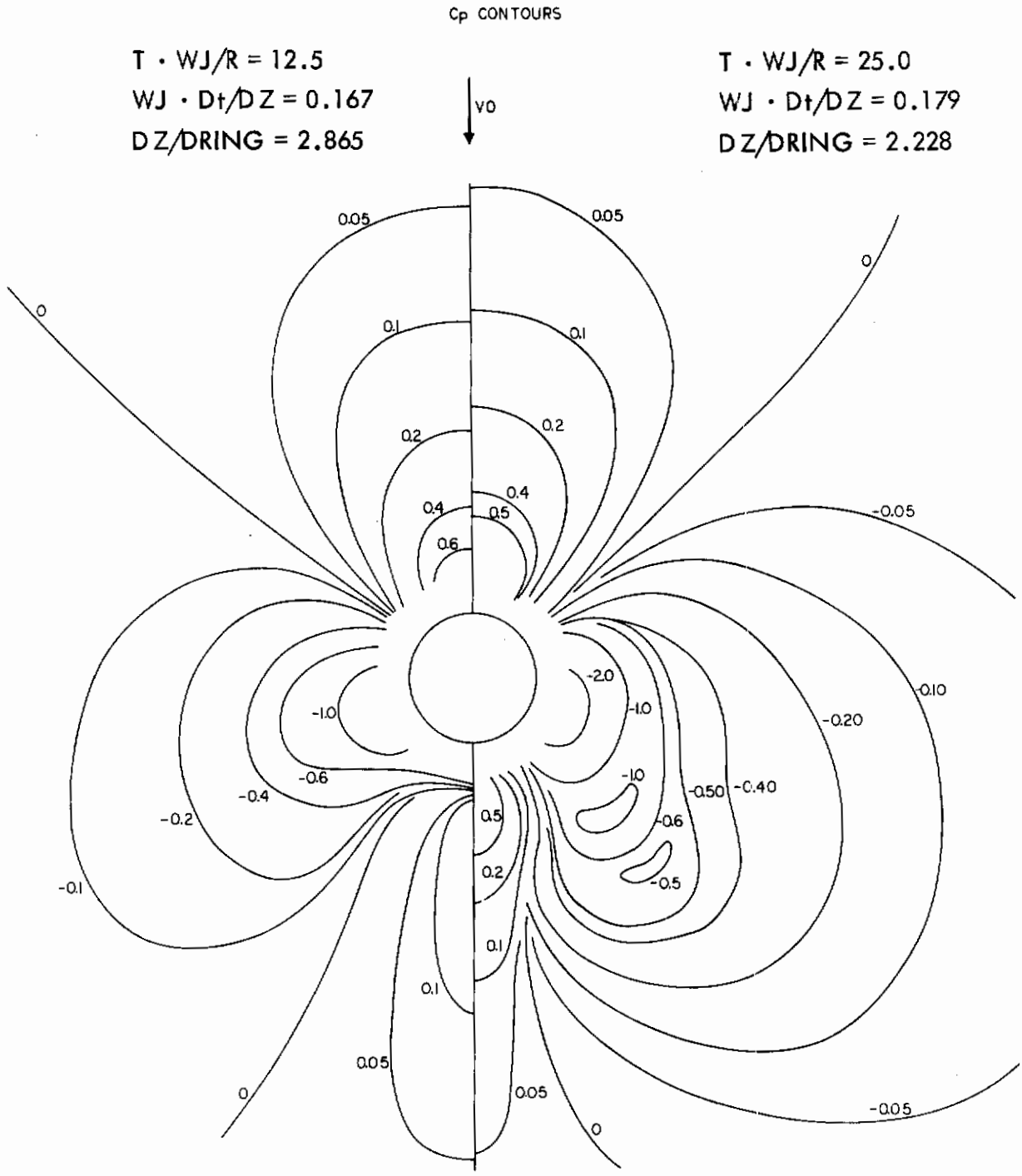

FIGURE 20. TIME HISTORY OF PRESSURE DISTRIBUTION FOR VO/WJ = 0.3

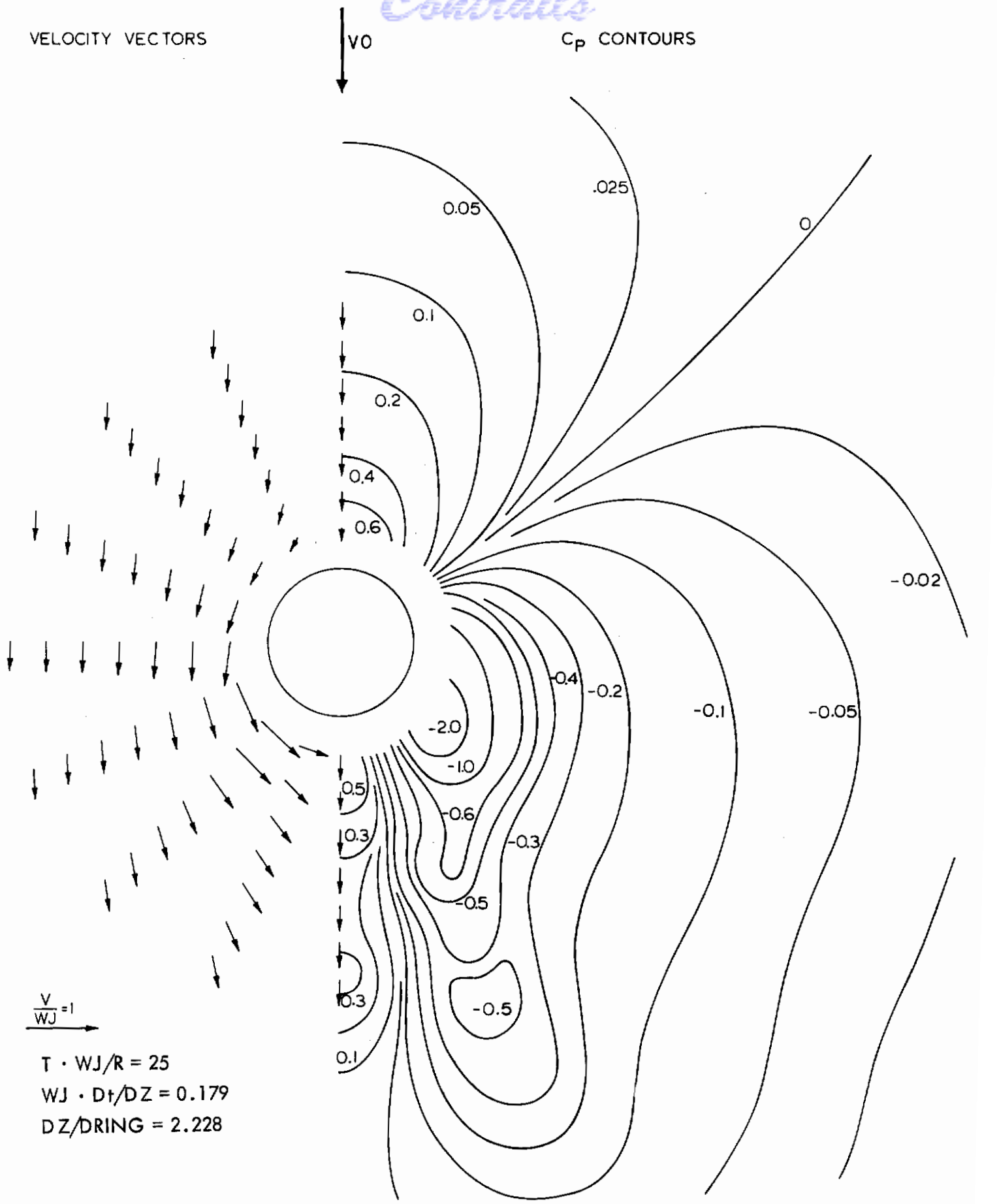

FIGURE 21. EXIT PLANE VELOCITY AND PRESSURE DISTRIBUTION FOR VO/WJ = 0.4

SECTION VII

CONCLUSIONS

A finite-element potential-flow modeling method has been programmed which predicts, without empiricism from experimental results, both the rolled-up geometry and the path of a round, lifting jet emergent at 90 degrees into a crossflowing mainstream, as on VTOL or direct-lift-assisted STOL aircraft. A combination of perturbation and collocation methods is necessary to accommodate the three-dimensional mixed "hard" and free-surface boundary conditions. An elementary reflection method, originally suggested for exit-plane simulation, could not be modified properly to allow for the jet exit hole. Consequently, it was necessary to devise collocation routines which impose both exit-plane and duct-suface, flow-tangency conditions. In tum, this allowed a more realistic simulation of duct effects, particularly the total pressure rise at the fan (at a chosen position) and acceleration of jet fluid inside the duct toward the low-pressure region near the back at the exit plane. Duct wall pressures are implicitly available but have not been determined.

An inherent difficulty for three-dimensional time-dependent finite-element solutions lies in the interpretation of results: not only position in space but local velocities and accelerations give valuable insight into the fluid mechanics. Computer-graphics technizues were found to be an almost indispensable aid in this regard and speeded both program checkout and experiments on the fluid mechanical aspects of the simulation.

Calculations have been made for various combinations of assumed initial geometry and circulation strengths, the best seems to be a circular cylinder sloped at an angle dependent on velocity ratio with circulation values equal to or somewhat less than a two-dimensional cylinder. Iteration using the collocation scheme moved the vortex strength peaks rearwards and intensified them. Three or four perturbation/collocation cycles were generally sufficient. However, care was necessary at the lower forward speeds because of a tendency of the jet to "flap" like a hose-end when freed. It seems that the open-end of the vortex tube, which resulted from ring removal to compensate for additons at the fan, has this inherent property. More gradual ring-strength attenuation — as in a real decaying jet — would at least alleviate this problem. It should be noted, however, that real jets do tend to "flap" somewhat, but this is an unwanted solution in the present context.

Pressure distributions calculated at the exit plane, after the plume distortion had occurred, showed many of the features seen in real flows except, of course, the more-constant pressure tendency of the separated bubble downstream of the orifice, which is not within the scope of the present potential flow approach. Nevertheless, for forward speed ratios between 0.1 and 0.4, the low-pressure lobes did show a rearward shift and intensification, just as is found experimentally.

Generally speaking, too little time has been spent running the programs described here, particularly in developing appropriate strategies for combining perturbation and collocation techniques. This has been due to the addition of more detailed collocation routines than originally conceived, although these do bring the application to practical aircraft geometries considerably closer. However, further work on the basic fluid mechanics, to include at least the major viscous features, should be attempted first.

APPENDIX

TWO FUNDAMENTAL RESULTS

Flow Inside a Cylinder Normal to a Mainstream

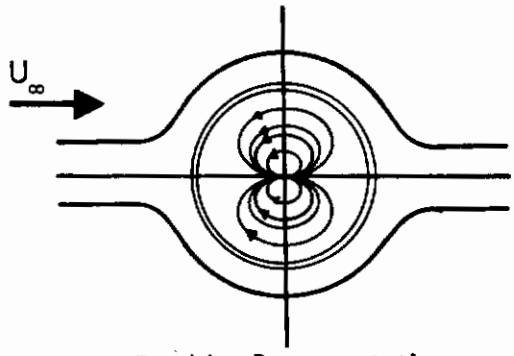

Doublet Representation

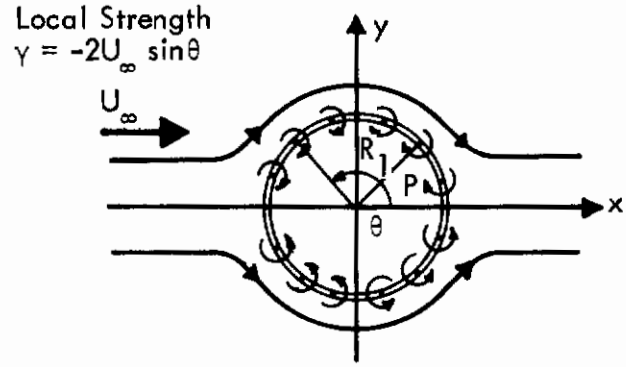

Vortex Sheet Representation

The sketches above illustrate a doublet and a vortex sheet representation of flow inside a cylinder normal to a mainstream. We wish to determine the velocity components, u,v, at point $P(r,\varphi)$ due to the vortex sheet at the surface of the cylinder.

On the cylinder, we may put $z = R_1 e^{i\theta}$ so that

$$dz = iR_1 e^{i\theta}\, d\theta = iz\,d\theta$$

and

$$\sin\theta = \frac{1}{2i}\left(e^{i\theta} - e^{-i\theta}\right) = \frac{1}{2i}\left(\frac{z}{R_1} - \frac{R_1}{z}\right)$$

also, putting $z_o = re^{i\varphi}$, we have

$$R = \left(R_1^2 + r^2 - 2R_1\, r\cos(\theta - \varphi)\right)^{1/2} \equiv R_1 e^{i\theta} - re^{i\varphi}$$

$$\equiv z - z_o$$

Now

$$dq = i\,\frac{\gamma R_1\, d\theta}{2\pi R} \qquad \gamma = -2U_\infty \sin\theta$$

$$= i\,\frac{-2U_\infty \frac{1}{2i}\left(\frac{z}{R_1} - \frac{R_1}{z}\right) R_1\, dz}{2\pi(z - z_o)\, iz}$$

Integrating around the circle,

$$q = -u + iv = \frac{-U_\infty}{2\pi} \int_c \frac{dz}{(z - z_o)} + \frac{U_\infty}{2\pi} i \int_c \frac{R_1^2\, dz}{z^2(z - z_o)}$$

$$= \frac{-U_\infty}{2\pi} i \left\{ 2\pi i - R_1^2\, 2\pi i \left(\frac{1}{z_o^2} - \frac{(-1)}{z_o^2} \right) \right\}$$

$$= + U_\infty$$

$$\therefore \quad u = -U_\infty \quad v = 0$$

Adding the mainstream component, we obtain for the interior of the cylinder,

$$\underline{u = 0 \qquad v = 0}$$

The above result may also be inferred by considering the rheoelectric analog for the flow. If the positive electrode is a horizontal strip at infinity above the cylinder and the negative one is at infinity below, the outline of the circle may be formed from a line conductor. Outside the cylinder equal voltage lines will then correspond to the streamlines as shown. Inside the cylinder, there can be no current flow and no potential differences. This corresponds to totally stagnant flow inside the cylinder.

The Flow Field of a Ring-Vortex Cylinder

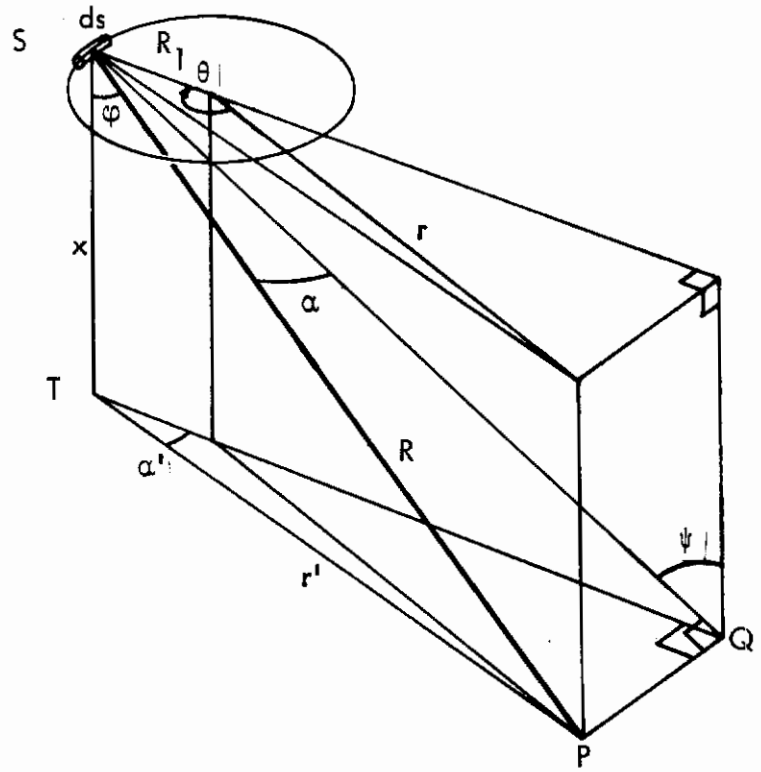

The preceding sketch shows one ring, representative of a vertical stack of rings, which forms a doubly infinite cylinder with centerline along the z axis. We shall consider a surface element with dimensions ds peripherally and dz axially and express the vortex strength as $\partial K/\partial z$, where the units of the circulation K are ft^2/sec.

Using the Biot-Savart law for the effect of an element at S on the point P, the total velocity becomes

$$dq = \frac{(\partial K/\partial z)\cos\alpha \, ds \, dz}{4\pi R^2}$$

The vertical component is

$$dw = dq \sin\psi = \frac{1}{4\pi R^2}\frac{\partial K}{\partial z}\cos\alpha \sin\psi \, ds \, dz$$

We shall integrate with respect to φ for the vertical direction and with respect to α' for horizontal planes, having the limits general. Now

$$ds = \frac{r' d\alpha'}{\cos\alpha'}$$

also

$$\cos\alpha = \frac{\sin\varphi}{\sin\psi}\cos\alpha'$$

and

$$R = r' \operatorname{cosec}\varphi$$

$$-z = R\cos\varphi = r' \operatorname{cosec}\varphi \cos\varphi = r' \cot\varphi$$

$$dz = r' \operatorname{cosec}^2\varphi \, d\varphi$$

Thus, the integral equation for the vertical component becomes

$$w = \frac{1}{4\pi}\int_{\alpha=\tilde{\alpha}_1}^{\tilde{\alpha}_2}\int_{\varphi=\Phi_1}^{\Phi_2}\frac{\sin^2\varphi}{r_1'^2}\left(\frac{r'}{\cos\alpha'}\right)\left(\frac{\sin\varphi}{\sin\psi}\cos\alpha'\right)\frac{\partial K}{\partial z}(\sin\psi)\left(\frac{-r'}{\sin^2\varphi}d\varphi\right)d\alpha'$$

Clearing yields

$$w = -\frac{1}{4\pi}\frac{\partial K}{\partial z}\int_{\tilde{\alpha}_1}^{\tilde{\alpha}_2}\int_{\Phi_1}^{\Phi_2}(\sin\varphi)d\varphi \, d\alpha'$$

$$\therefore \quad w = \frac{1}{4\pi}\frac{\partial K}{\partial z}\int_{\tilde{\alpha}_1}^{\tilde{\alpha}_2} [\cos\varphi]_{\Phi_1}^{\Phi_2}\, d\alpha'$$

$$= \underline{\underline{\frac{1}{4\pi}\frac{\partial K}{\partial z}(\cos\Phi_2 - \cos\Phi_1)(\tilde{\alpha}_2 - \tilde{\alpha}_1)}}$$

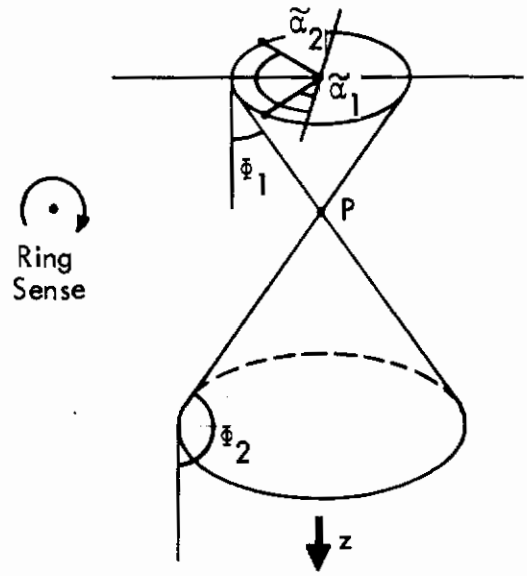

As shown in the above sketch, the limits $\Phi_1, \Phi_2, \tilde{\alpha}_1, \tilde{\alpha}_2$ in spherical coordinates describe a segment intersecting two cones which has a plan-view included angle of $(\tilde{\alpha}_2 - \tilde{\alpha}_1)$. The cones have surface angles Φ_1 and Φ_2, as shown. Though these spherical coordinates are of limited use in general, three useful results can be obtained for doubly infinite cylinders, with P inside the cylinder, on the boundary and outside, respectively.

P inside the boundary of a closed, doubly infinite cylinder

$$\tilde{\alpha}_1 = \pi \qquad \tilde{\alpha}_2 = -\pi \qquad \Phi_1 = 0 \qquad \Phi_2 = \pi$$

$$w = \frac{1}{4\pi}\frac{\partial K}{\partial z}(-1 - (+1))(-\pi - (+\pi)$$

$$= \frac{\partial K}{\partial z}$$

P on the surface of a closed, doubly infinite cylinder

$$\tilde{\alpha}_1 = +\frac{\pi}{2} \qquad \tilde{\alpha}_2 = -\frac{\pi}{2} \qquad \Phi_1 = 0 \qquad \Phi_2 = \pi$$

$$w = \frac{1}{4\pi}\frac{\partial K}{\partial z}(-1 - (+1))\left(-\frac{\pi}{2} - (+\pi/2)\right)$$

$$= \frac{1}{2}\frac{\partial K}{\partial z}$$

P outside the boundary of a closed, doubly infinite cylinder

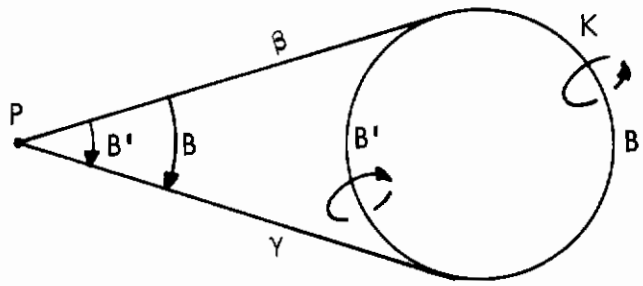

Segment ABC $\tilde{\alpha}_1 = \beta$ $\tilde{\alpha}_2 = \gamma$ $\Phi_1 = 0$ $\Phi_2 = \pi$

Segment AB'C $\tilde{\alpha}_1 = \gamma$ $\tilde{\alpha}_2 = \beta$ $\Phi_1 = 0$ $\Phi_2 = \pi$

For Segment ABC plus AB'C

$$w = \frac{1}{4\pi}\frac{\partial K}{\partial z}(-1 - (+1))((\beta - \gamma) + (\gamma - \beta))$$
$$= 0$$

It is evident from considerations of symmetry (or from continuity) that no radial or peripheral flows are induced in the system.

Symmetry yields the same result for semi-infinite cylinders, but it applies only in the plane of the cut end where the axial velocities equal half the corresponding values given above. However, radial velocities are now also present in this plane and, at the cut end itself, there is a radial-flow singularity analogous to the familiar wing-tip singularity.

REFERENCES

1. L. J. S. Bradbury and M. N. Wood, "The Static Pressure Distribution around a Circular Jet Exhausting Normally from a Plane Wall into an Airstream," R.A.E. Tech Note Aero 2978, August 1964.

2. R. D. Vogler, "Surface Pressure Distributions Induced on a Flat Plate by a Cold Air Jet Issuing Perpendicularly from the Plate Normal to a Low-Speed Free-Stream Flow," NASA TN D-1629.

3. R. Jordinson, "Flow in a Jet Directed Normal to the Wind," R and M No. 3074, British ARC, 1958.

4. R. J. Margasson, "The Path of a Jet Directed at Large Angles to a Subsonic Free Stream," NASA TND-4919, 1968.

5. "Analysis of a Jet in a Subsonic Crosswind," (Symposium Proceedings) NASA SP-218, September 1969.

6. Hsui-Chen Chang-Lu, "Aufrollung eines Zylindrischen Strahles durch Querwind" (Roll-Up of a Cylindrical Jet in a Crosswind), Doctoral Dissertation, University of Gottingen, 1942.

   See also:

   H. C. Lu, "On the Surface of Discontinuity between Two Flows Perpendicular to Each Other," Nat. Tsing Hua University Eng. Rep. 4,1, October 1948, pages 40-62.

7. T. E. Base and J. E. Hackett, "Analysis of Vortex Ring Representation by Finite Elements," Lockheed-Georgia Research Memorandum ER-10331, October 1969.

UNCLASSIFIED
Security Classification

DOCUMENT CONTROL DATA - R&D
(Security classification of title, body of abstract and indexing annotation must be entered when the overall report is classified)

1. ORIGINATING ACTIVITY *(Corporate author)*
Lockheed-Georgia Company
A Division of Lockheed Aircraft Corporation
Marietta, Georgia

2a. REPORT SECURITY CLASSIFICATION
UNCLASSIFIED

2b. GROUP

3. REPORT TITLE
A THEORETICAL INVESTIGATION OF A CIRCULAR LIFTING JET IN A CROSS-FLOWING MAINSTREAM

4. DESCRIPTIVE NOTES *(Type of report and inclusive dates)*
Final Report, July 1969 - December 1970

5. AUTHOR(S) *(Last name, first name, initial)*
Hackett, James E.
Miller, H. Ronald

6. REPORT DATE	7a. TOTAL NO. OF PAGES	7b. NO. OF REFS
January 1971	49	7

8a. CONTRACT OR GRANT NO.	9a. ORIGINATOR'S REPORT NUMBER(S)
F33615-69-C-1753	
b. PROJECT NO. 6169BT	AFFDL-TR-70-170
c.	9b. OTHER REPORT NO(S) *(Any other numbers that may be assigned this report)*
d.	

10. AVAILABILITY/LIMITATION NOTICES
This document has been approved for public release and sale; its distribution is unlimited.

11. SUPPLEMENTARY NOTES	12. SPONSORING MILITARY ACTIVITY
	Air Force Flight Dynamics Laboratory Air Force Systems Command Wright-Patterson Air Force Base, Ohio

13. ABSTRACT

Finite-element potential-flow-modeling theoretical techniques are described which predict, from first principles, both the rolled-up geometry and the path of a round lifting jet convergent into a cross-flowing mainstream, as on VTOL or direct lift-assisted STOL aircraft. Starting with a straight-cylinder geometry, "point" vortex elements are perturbed using a predictor-corrector stepping method to give a first estimate of the bent-back shape, using assumed circulation values. A collocation scheme is next used to revise the circulation values, and after three or four iterations, a final exit-plane pressure distribution may be calculated. The fan-induced total pressure rise is simulated by injecting vortex rings at a chosen position in the duct which feeds the jet. Since the scope of the method is entirely non-viscous, separations toward the rear of real jets and the associated pressure changes are not simulated and base-pressure type of pressures cannot be expected. Nevertheless, for forward speed ratios of 0.1, 0.2, 0.3 and 0.4, the low-pressure contours at each side of the jet do show an increasing rearward shift, just as is found experimentally. Somewhat surprisingly, the simulated plumes were more stable at higher velocity ratios. At lower forward speeds, there was a tendency to flap, rather like a hose end when freeds. It is anticipated that, if viscous effects were simulated, these motions might damp out.

DD FORM 1 JAN 64 1473

UNCLASSIFIED
Security Classification

14. KEY WORDS	LINK A		LINK B		LINK C	
	ROLE	WT	ROLE	WT	ROLE	WT
Finite element method Jet in cross flow Vortices Jet interaction Potential Flow Aerodynamic Modeling Jet Flow V/STOL aerodynamics Computer Programs						

INSTRUCTIONS

1. ORIGINATING ACTIVITY: Enter the name and address of the contractor, subcontractor, grantee, Department of Defense activity or other organization *(corporate author)* issuing the report.

2*a*. REPORT SECURITY CLASSIFICATION: Enter the overall security classification of the report. Indicate whether "Restricted Data" is included. Marking is to be in accordance with appropriate security regulations.

2*b*. GROUP: Automatic downgrading is specified in DoD Directive 5200.10 and Armed Forces Industrial Manual. Enter the group number. Also, when applicable, show that optional markings have been used for Group 3 and Group 4 as authorized.

3. REPORT TITLE: Enter the complete report title in all capital letters. Titles in all cases should be unclassified. If a meaningful title cannot be selected without classification, show title classification in all capitals in parenthesis immediately following the title.

4. DESCRIPTIVE NOTES: If appropriate, enter the type of report, e.g., interim, progress, summary, annual, or final. Give the inclusive dates when a specific reporting period is covered.

5. AUTHOR(S): Enter the name(s) of author(s) as shown on or in the report. Enter last name, first name, middle initial. If military, show rank and branch of service. The name of the principal author is an absolute minimum requirement.

6. REPORT DATE: Enter the date of the report as day, month, year; or month, year. If more than one date appears on the report, use date of publication.

7*a*. TOTAL NUMBER OF PAGES: The total page count should follow normal pagination procedures, i.e., enter the number of pages containing information.

7*b*. NUMBER OF REFERENCES: Enter the total number of references cited in the report.

8*a*. CONTRACT OR GRANT NUMBER: If appropriate, enter the applicable number of the contract or grant under which the report was written.

8*b*, 8*c*, & 8*d*. PROJECT NUMBER: Enter the appropriate military department identification, such as project number, subproject number, system numbers, task number, etc.

9*a*. ORIGINATOR'S REPORT NUMBER(S): Enter the official report number by which the document will be identified and controlled by the originating activity. This number must be unique to this report.

9*b*. OTHER REPORT NUMBER(S): If the report has been assigned any other report numbers *(either by the originator or by the sponsor)*, also enter this number(s).

10. AVAILABILITY/LIMITATION NOTICES: Enter any limitations on further dissemination of the report, other than those imposed by security classification, using standard statements such as:

(1) "Qualified requesters may obtain copies of this report from DDC."

(2) "Foreign announcement and dissemination of this report by DDC is not authorized."

(3) "U. S. Government agencies may obtain copies of this report directly from DDC. Other qualified DDC users shall request through _____."

(4) "U. S. military agencies may obtain copies of this report directly from DDC. Other qualified users shall request through _____."

(5) "All distribution of this report is controlled. Qualified DDC users shall request through _____."

If the report has been furnished to the Office of Technical Services, Department of Commerce, for sale to the public, indicate this fact and enter the price, if known.

11. SUPPLEMENTARY NOTES: Use for additional explanatory notes.

12. SPONSORING MILITARY ACTIVITY: Enter the name of the departmental project office or laboratory sponsoring *(paying for)* the research and development. Include address.

13. ABSTRACT: Enter an abstract giving a brief and factual summary of the document indicative of the report, even though it may also appear elsewhere in the body of the technical report. If additional space is required, a continuation sheet shall be attached.

It is highly desirable that the abstract of classified reports be unclassified. Each paragraph of the abstract shall end with an indication of the military security classification of the information in the paragraph, represented as *(TS), (S), (C), or (U)*.

There is no limitation on the length of the abstract. However, the suggested length is from 150 to 225 words.

14. KEY WORDS: Key words are technically meaningful terms or short phrases that characterize a report and may be used as index entries for cataloging the report. Key words must be selected so that no security classification is required. Identifiers, such as equipment model designation, trade name, military project code name, geographic location, may be used as key words but will be followed by an indication of technical context. The assignment of links, rules, and weights is optional.

GPO 886-551